AD-A056 145 BRITISH COLUMBIA UNIV VANCOUVER INST OF OCEANOGRAPHY F/G 8/10
A SYSTEM FOR REMOTE MEASUREMENTS OF AIR-SEA FLUXES OF MOMENTUM,--ETC(U)
MAR 78 S POND, W G LARGE N00014-76-C-0446
UNCLASSIFIED IOUBC-MS-32 NL

1 OF 1
AD
A056 145

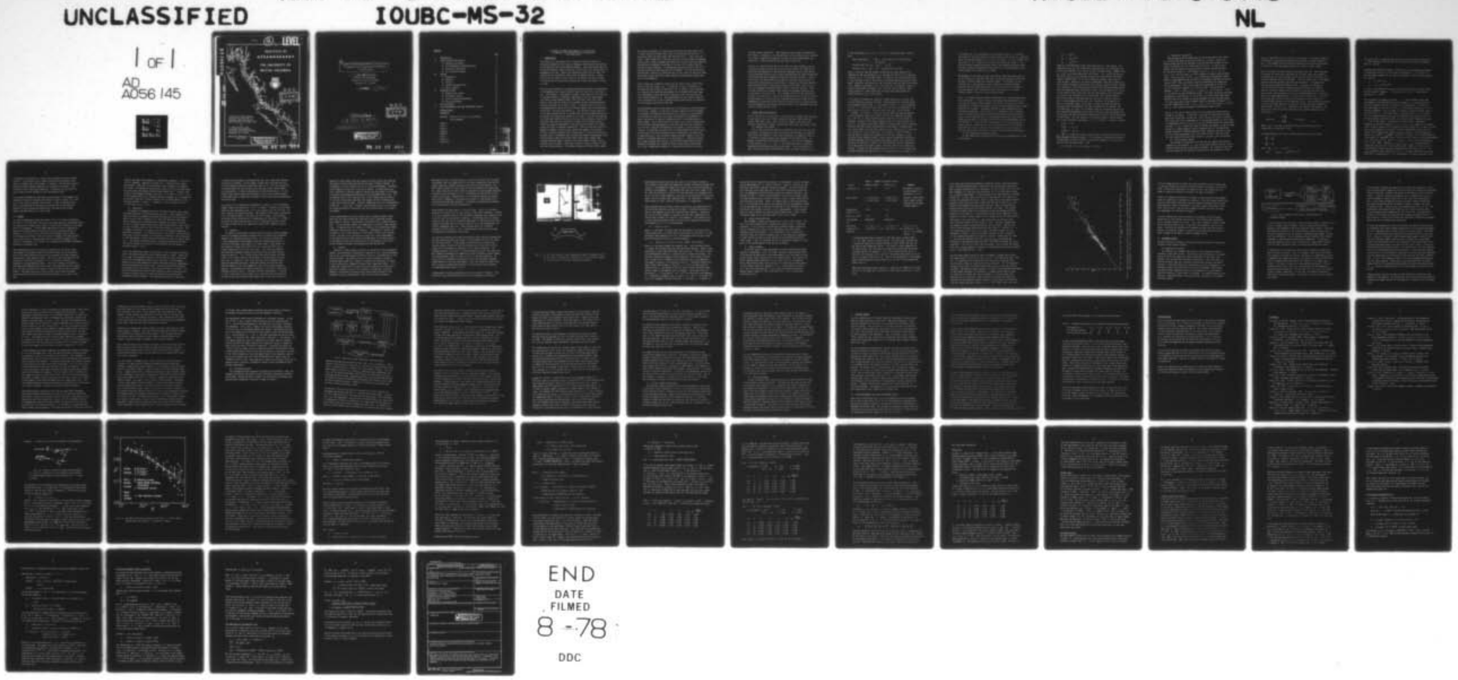

END
DATE
FILMED
8-78
DDC

INSTITUTE OF OCEANOGRAPHY

THE UNIVERSITY OF BRITISH COLUMBIA

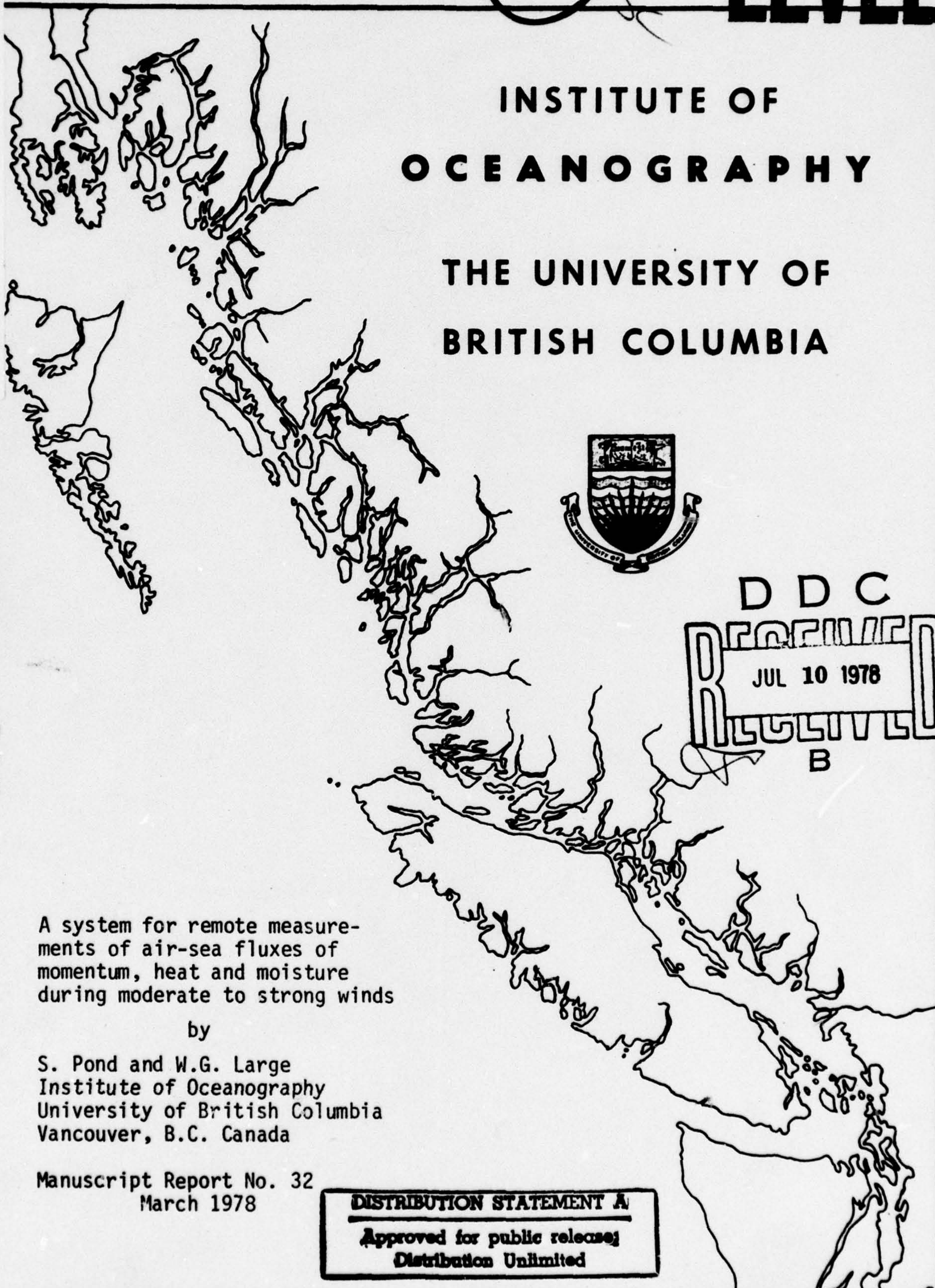

A system for remote measurements of air-sea fluxes of momentum, heat and moisture during moderate to strong winds

by

S. Pond and W.G. Large
Institute of Oceanography
University of British Columbia
Vancouver, B.C. Canada

Manuscript Report No. 32
March 1978

(6)

A system for remote measurements of air-sea fluxes of momentum, heat and moisture during moderate to strong winds.

(10) S. Pond [redacted] W.G. Large
Institute of Oceanography
University of British Columbia
Vancouver, B.C. Canada

(11) Mar[redacted]978 (12) 56p.

(9) Manuscript Report No. 32

(14) IOUBC-MS-32

(15) N00014-76-C-0446

CONTENTS

A system for remote measurements of air-sea fluxes of momentum, heat and moisture during moderate to strong winds

I. INTRODUCTION

This report is a description of an internally recording system for obtaining estimates of the fluxes of momentum, sensible heat and moisture by the Reynolds flux and dissipation methods. While these techniques are not new an automatic system using them is novel and so is the way the Gill anemometers are used. Some of the techniques should also be useful for acquisition and recording of other kinds of geophysical data. Before describing the system, a brief review of the reasons why such a system is required and of the existing information on which the design is based is given.

Over the past ten years or so there have been many reports of measurements of the momentum flux, some of sensible heat flux and a few of moisture flux. While there is considerable scatter in each data set for a variety of possible reasons, a reasonably consistent picture for the momentum flux seems to have emerged (Hidey, 1972; Phillips, 1972; Pond, 1975; Stewart, 1974) over the range of wind speeds for which good measurements have been obtained (up to about 15 m/s). It appears that this flux can be parameterized in terms of the wind speed squared with a non-dimensional coefficient - the drag coefficient, C_D. For the other fluxes there are not so many observations but it appears that similar parameterizations may be possible for them as well (Pond, et al., 1974). Even for the momentum flux there are insufficient data to try to pick out particular sources of variation within the real statistical scatter such as those caused by stability, stage of development of the wave field, presence of a frontal system, and lack of complete stationarity. There are also two schools of thought on whether or not the drag coefficient depends on wind speed. Phillips (1972) and Stewart (1974) suggest that, in view of the scatter, a constant value is reasonable over the existing range of measurements while Smith and Banke (1975) and Garrett (1977) among others suggest some increase with wind speed. Because of the small amount of data, such an increase could be found in some sets of data or could be missed in other sets due to other factors. For example, Denman and Miyake (1973) suggest that during conditions of increasing wind velocity the drag coefficient is higher because the wave field is not in equilibrium with the wind. In decreasing winds one might expect the opposite effect. In any case, the trend is small enough that it probably would have little effect on computed average stress values, provided that winds over 15 m/s do not make important contributions, although calculations of the curl of the stress might be affected by the difference. If the present data gave results to 20 m/s it would be possible to make more definite statements. For the stress vector averaged over a month or so there are few, if any, places on the world ocean where winds greater than 20 m/s make important contributions because they occur too infrequently.

Clearly there are a number of reasons why one would like to collect more data to calculate values of C_D. In addition, if one is interested in following the time history of the stress and its effects, then it becomes very important to extend the measurements to the higher wind speed range. Such measurements should settle the controversy over the trend and give a much better measure of it. More measurements of the fluxes of sensible heat and moisture and of their parameterization coefficients are needed at all wind speeds, particularly high ones.

Such measurements have not been obtained so far because of the experimental difficulties. However, it should be possible, because of the development of techniques for obtaining the necessary data, because of the knowledge of the nature of quantities now gained, and because of developments in modern electronics, to design a system which will allow measurements at higher speeds. One of the serious difficulties is to find a suitable platform from which such measurements can be made under open sea conditions. For the 'best' technique (the Reynolds flux method) a stable platform is required. In addition, one would like to develop methods which would work on more readily available platforms such as weatherships and other ships of opportunity (e.g. the dissipation method, provided comparison with the Reynolds flux method shows that it is satisfactory). Internal recording would seem to be desirable because any suitable stable platforms would probably be unmanned (for reasons of safety, among others) and because for a ship of opportunity program it is much more efficient not to have to send a team of observers. Some compromises would have to be made with this choice. Telemetry is an alternative, but would probably not be suitable for a ship of opportunity program, increases the power requirements substantially, is more complicated and has range limitations.

Finally, it is worth noting that to be useful for other purposes, such as calculating fluxes over the world ocean or parts thereof for modeling and predicting the behaviour of the ocean and atmosphere, more or less direct flux observations must be used to obtain parameterizations that estimate the fluxes from more easily measured and readily available variables. More or less direct flux observations are simply too difficult and too costly to be made over wide areas on a routine basis. Generally, the direct measurements have been used to examine and evaluate coefficients, such as C_D, in the bulk aerodynamic parameterization (given in the next section). Even the data required to estimate fluxes using this parameterization are not as available as one would like. Thus another part of air-sea interaction research to be pursued is a search for parameterizations in terms of readily available data, e.g. wind roses and long-term average sea surface and air temperatures and humidities for long-term average fluxes or surface pressure maps and temperature and humidity values to look at time dependent processes (Fissel, Miyake and Pond, 1977).

II. THEORY AND EXISTING RESULTS

Only an outline will be given here as more detailed treatments are available in many sources (e.g. Roll, 1965; Lumley and Panofsky, 1964; Monin and Yaglom, 1965, 1967; Kraus, 1972; Burling and Stewart, 1967; Busch and Panofsky, 1968; Miyake, Stewart and Burling, 1970; Pond, 1975; Busch, 1977).

a) Reynolds flux method -

This is the most direct method of estimating the fluxes and, with the development of techniques to make the necessary measurements, is generally taken to be the standard to which other techniques are compared directly, or indirectly through comparison of parameterization coefficients. It depends on measuring the covariance between w, the vertical component of the velocity, and U, T and q, the downstream velocity component, temperature and absolute humidity, respectively. Since the average of $w(\overline{w})$ must be zero (Burling and Stewart, 1967), the total values (U,T,q)

or the fluctuations ($u = U - \overline{U}$, $T' = T - \overline{T}$, $q' = q - \overline{q}$) may be used. Thus we have:

Stress magnitude, $\tau = -\rho\ \overline{Uw} = -\rho\ \overline{uw}$ and acts in the direction of the wind

Sensible heat flux, $H_S = \rho C_p\ \overline{wT} = \rho C_p\ \overline{wT'}$

Moisture flux, $E = \overline{wq} = \overline{wq'}$ = (latent heat flux, H_L)/L

where ρ is the air density (whose fluctuations are small enough to be neglected in the calculations), C_p is the specific heat of air at constant pressure, and L is the latent heat. In practice, one must make sure that w does not have a mean or large trends introduced spuriously by the instruments. Generally, one should use the variations about the mean of the record used. Whether to detrend or not is not clear-cut. Personally, unless we suspect considerable instrument drift, we prefer not to detrend. Other groups always do. Either method may introduce some unmeasurable but hopefully small errors in the results.

It is useful to examine the cospectra of these quantities to ensure that all contributions are being included. Contributions occur over the normalized frequency range, $0.001 < n < 10$, where $n = fZ/\overline{U}$, f is the frequency (in Hz), Z is the observation height (in m) and $\overline{U}$ is the magnitude of the mean velocity (in m/sec). Thus one should work with a record length $T \approx 1000Z/\overline{U}$. In practice, a few such records should be averaged together to get reasonable statistical stability of the low frequency estimates. E.g., for $Z/\overline{U} \approx 1$, four 15-minute records or an hour of data should be adequate. Because of the large frequency range it is usual to plot log f or log n. To obtain a plot whose integral is proportional to the covariance and such that the relative contributions from different frequency bands are clearly shown, one then plots frequency times cospectrum, C_o, since then $2.3f\ C_o\ d(\log f) = C_o\ df$, and the $\int_0^\infty \propto$ covariance. In the following, when we refer to spectra and cospectra we shall mean frequency x these variables unless otherwise noted. These cospectra normalized according to the Monin-Oboukhov similarity theory and plotted against log n should be functions of stability. However, for the stabilities usually encountered at sea and within the natural scatter, stability effects can probably be ignored. The peaks of the cospectra occur for $0.01 < n < 0.1$ in most cases although sometimes the peak of the wT cospectrum occurs at values of n up to about 0.5. The contribution to the cospectra from $n > 1$ is only a few percent of the total except for these unusual cases of the wT cospectrum where the contribution may be up to 20% of the total. It is now thought that these cases of wT cospectra with large contributions at larger n are spurious results caused by moisture films on the temperature sensors which introduce large errors when the latent heat flux is large compared to the sensible heat flux (Friehe, et al., 1976).

Measurements of this type are made some distance above the surface but it is not difficult to show that the fluxes are nearly constant for the first few tens of metres (Lumley and Panofsky, 1964). The thickness of this 'constant flux' layer generally should increase with the wind speed. Assuming that the normalized cospectra will not be grossly different at high wind speeds, this information allows one to work out a suitable sampling scheme in terms of rate and record length.

While it is perhaps the best method, the Reynolds flux technique does have some limitations. In order to obtain the cospectra to ensure that the covariances are correct one must sample at a fairly fast rate for a fairly long time, so a rather large amount of data must be recorded to get a single Reynolds flux estimate. The method requires a known, preferably fixed, instrument orientation. In principle, it is possible to use a platform such as a surface ship, measure the motion and make corrections point by point. Such an approach makes the measurement program much more complicated and thus makes it even more difficult to obtain measurements one can be confident in. As the problem at high speeds is difficult enough on a stable platform it seems best to use such a platform, at least initially. One might also look for and test other methods at the same time which could be used on mobile platforms and have reduced recording requirements.

b) Bulk aerodynamic parameterizations

In this method one assumes that the fluxes may be parameterized in the following way:

$$|\vec{\tau}| = \rho C_D \overline{U}^2$$

$$H_S = \rho C_p C_T \overline{U}\Delta T$$

$$H_L = C_q \overline{U}\Delta q \cdot L$$

where $\overline{U}$ is the magnitude of the vector mean wind, ΔT = sea surface - air temperature, and Δq = sea surface-air humidity and $\overline{U}$, air temperature and humidity are measured at or reduced to some reference height, commonly 10 m; C_D, C_T and C_q are non-dimensional coefficients. C_D is called the drag coefficient; C_T and C_q are sometimes referred to as the Stanton and Dalton numbers, respectively. $\overline{U}$, ΔT and Δq should be averages over times of order an hour. Generally, sea surface temperatures (and hence humidity at the surface) are based on occasional spot readings, usually 'bucket' samples. Spot readings or fairly short averages (the usual ship observations) may be used with some additional statistical scatter since the means of $\overline{U}$, ΔT and Δq are generally much larger than the root mean square (rms) fluctuations. To calculate the parameterization coefficients, $|\overline{\vec{U}}|$, the magnitude of vector mean wind, or the mean speed over the record length of about an hour, is used depending on the data set. Normally, for periods of an hour or so the mean speed is less than 1% higher than the magnitude of the vector mean (see Appendix) and the differences can be ignored. One can examine C_D, C_T, and C_q to see whether they are reasonably constant or have measurable dependence on wind speed, stability, wave development, etc. One can also use these formulae to estimate the ratios of scaling amplitudes to mean values. For this purpose, to set design criteria without making any claim to exactness, we take $C_D \sim C_T \sim C_q \sim (1/25)^2 = 1.6 \times 10^{-3}$. We put

$$C_D \overline{U}^2 = u_*^2$$

$$C_T \overline{U}\Delta T = \kappa u_* T_*$$

$$C_q \overline{U}\Delta q = \kappa u_* q_*$$

$u_* = |\overline{uw}|^{1/2}$ is called the friction velocity and is the velocity scale of the Monin-Oboukhov similarity theory. κ is von Karman's constant ($\simeq 0.4$) and is included here in the definition of the scaling parameters T_* and q_* as is usually (but not always) done. Then

$$u_* \cong 1/25\ \overline{U},\ T_* \cong 1/10\ \Delta T \text{ and } q_* \cong 1/10\ \Delta q.$$

c) Statistical quantities

Here we want to relate amplitudes of the fluctuations to the scales u_*, T_* and q_* and hence to the mean values, $\overline{U}$, ΔT and Δq. Again, we present values that do not necessarily provide the final answer but are useful for design, e.g. for picking amplifier gains. We tend to pick numbers near the high end of existing data to avoid overload problems. We look at rms values $\sigma_\alpha = (\overline{\alpha^2})^{\frac{1}{2}}$ where α may be u, w, T' or q'. $\sigma_w/u_* \sim 1.2 - 1.5$ so we take $\sigma_w \approx 0.06\ \overline{U}$, perhaps a slightly high estimate. $\sigma_u/u_* \sim 2.5$ so we use $\sigma_u = 0.1\ \overline{U}$. σ_u/u_* values show considerable scatter which is associated with the fact that low frequencies dominate the contributions to $\overline{u^2}$. Thus, the record length and detrending can change this value considerably. These values should be representative if the low cut off normalized frequency $n \sim 0.001$ to 0.002. The correlation between u and w, $-u_*^2/\sigma_u\sigma_w$ for $\sigma_w = 0.06\ \overline{U}$, $\sigma_u = 0.1\ \overline{U}$, and $u_* = 1/25\ \overline{U}$ is -0.27 which is close to observed values. All these ratios may have some dependence on stability but it is too small to be well established experimentally and can be ignored for design purposes over the expected range. σ_T/T_* and σ_q/q_* seem to have stronger stability dependence although it is not well established either. $\sigma_T/T_* \sim \sigma_q/q_* \sim \frac{1}{2}$ to 1 so we take $\sigma_T \sim 1/10\ \Delta T$ and $\sigma_q \sim 1/10\ \Delta q$ which we expect to be reasonable upper limits.

Clearly, since none of these numbers are very exact some leeway must be allowed in our design. In addition, if C_D does increase with wind speed some other things must increase too. Over land C_D's are usually considerably larger and fairly independent of $\overline{U}$ provided the geometry of the surface is independent of $\overline{U}$, but σ_u/u_* and σ_w/u_* and the $\overline{uw}$ correlation remain about the same. If C_D is higher over water at higher wind speeds, it may be simply because of a higher apparent surface roughness with all the properties scaled according to the Monin-Oboukhov theory remaining the same as they do for existing measurements over both land and water. One must allow for such a possibility and higher values of $\sigma_u/\overline{U}$ and $\sigma_w/\overline{U}$ in any design.

d) The dissipation method

This method of estimating the fluxes does not require the vertical component of the velocity, w, and is thus more suited for use on a ship or mobile platform than is the eddy flux method. It is based on the idea that the production of turbulent fluctuations in the velocity or scalar fields is balanced locally by molecular dissipation. In unstable conditions this balance in the kinetic energy equation includes a buoyant production term. This unstable case and possible approaches by which one may be able to allow for it are discussed by Pond et al. (1971) or Busch (1977).

Here, for brevity, we shall discuss the neutral case only. Over the ocean at moderate to strong winds the stability is almost always near neutral. Exceptions may occur over regions such as the Gulf Stream or Kuroshio with cold air outbreaks from the continents. There are other terms in the energy equations but the available data show that production ≈ dissipation for near neutral to moderately unstable cases. We expect this balance to continue to hold at high wind speeds (because according to the Monin-Oboukhov similarity theory, which rationalizes existing data over both sea and land, such relations are not wind speed dependent) but an essential part of our measurement program is to verify this expectation. If we find the balance does not hold, then we shall attempt to find an empirical correction which allows us to estimate the fluxes. (Our preliminary analysis of some of our data shows that C_D obtained from the dissipation method is statistically similar to C_D obtained by the Reynolds flux method.) For near neutral stability and stationary and horizontally homogeneous flow, the balance is:

$$\text{production} \begin{cases} = -\overline{uw}\,\dfrac{d\overline{U}}{dZ} = \\[2ex] = -\overline{w\gamma'}\,\dfrac{d\overline{\gamma}}{dZ} = \end{cases} \text{dissipation} \begin{cases} = \varepsilon \\[2ex] = N_\gamma \end{cases}$$

where $\overline{\gamma}$ and γ' are used to represent the mean and fluctuating part, respectively, of any scalar field.

The mean gradients are given by the Monin-Oboukhov similarity theory

$$\frac{d\overline{U}}{dZ} = \frac{u_*}{\kappa Z}$$

$$\frac{d\overline{\gamma}}{dZ} = \frac{\gamma_*}{Z}$$

Thus, $-\overline{uw} = u_*^2 = (\kappa\varepsilon Z)^{2/3}$

$$|\overline{w\gamma'}| = |\kappa u_* \gamma_*| = (\kappa Z)^{2/3}\, N_\gamma^{1/2}\, \varepsilon^{1/6}\,.$$

The sign of $\overline{w\gamma'}$ is given by the sign of the air-sea surface difference in γ. These equations allow estimates of the fluxes to be made from measurements of ε and N_γ.

Assuming that Kolmogoroff theory is applicable, the one dimensional spectra of downstream velocity (ϕ_u) and scalar fluctuations (ϕ_γ) for values of k, the downstream component of the radian wave number, in the inertial subrange are given by:

$$\phi_u = K' \varepsilon^{2/3} k^{-5/3}$$

$$\phi_\gamma = B_\gamma' N_\gamma \varepsilon^{-1/3} k^{-5/3}$$

K' and B_γ' are Kolmogoroff constants (0.55 and 0.8, Paquin and Pond, 1971), and the observed frequency f and mean wind $\overline{U}$ give k using Taylor's hypothesis ($k = 2\pi f/\overline{U}$).

The dissipation of mechanical energy, ε, is thus obtained solely from measurements of the downstream velocity component, U, provided that frequencies extending into the -5/3 range of ϕ_u are observed. In practice, this measurement is not too difficult, as a normalized frequency of $n > 0.2$ should be adequate. The -5/3 range, if isotropy is really required, should not start until $n > 1$, but empirically it extends back to $n \sim 0.2$ or even 0.1 for the downstream velocity and for temperature and humidity, which is fortunate because relatively simple robust sensors which respond fully past $n = 1$ are not available. Considerable platform motion is acceptable. [Supposed the measured component is $U\cos\delta + w\sin\delta + U_R$, where U_R is the additional velocity caused by the fluctuating platform motion and δ is the tilt into the wind (see Appendix). Provided we make our measurements outside the frequency range of the platform motion, U_R can be ignored. Then the measured spectrum is $\phi_u \overline{\cos^2\delta} + \phi_{uw} \overline{\sin 2\delta} + \phi_w \overline{\sin^2\delta}$, assuming δ is not correlated with u and w which is reasonable. Now $|\delta|$ should be fairly small so we get approximately $\phi_u(1 - \overline{\delta^2}) + 2\overline{\delta}\phi_{uw} + \overline{\delta^2}\phi_w$. With $|\overline{\delta}| \leq 5°$ and $\sigma_\delta = 10°$, a fairly extreme case, $|\overline{\delta}| \leq 0.1$, $\overline{\delta^2} \leq 0.05$. Further, $\phi_w \simeq \phi_u$ and $|\phi_{uw}| < \frac{1}{2}\phi_u$, so there may be a random error of up to 10% in this extreme case. Almost all of this error is associated with $\overline{\delta}$ which one would hope would not be as large as 5° in size. $|\phi_{uw}|/\phi_u$ depends quite strongly on n; for $n > 0.3$ where one would try to work this ratio $\leq \frac{1}{4}$ and the error $< 5\%$.] Measurement of a scalar variable in the

-5/3 range of its spectrum, ϕ_γ, gives the dissipation of scalar fluctuations N_γ. In principle, only a single discrete value from each of the spectra, averaged over a few minutes, is required. The recording requirements are greatly reduced compared to the Reynolds flux method. Time histories of the fluxes may be compiled. In practice, we use three frequency bands for each variable as will be discussed later.

The dissipation method has been shown to give values of the momentum flux comparable to those of the eddy flux method in several studies (e.g. Pond et al., 1971; Smith and Banke, 1975), mainly in light to moderate winds. Only a few comparisons of moisture and sensible heat fluxes from both Reynolds flux and dissipation methods have been made but the method appears feasible (Pond et al., 1971, 1974).

III. SENSORS

For work at moderate to high wind speeds (5 ms^{-1} or 10 knots to hopefully 30 - 40 ms^{-1} or 60 - 80 knots) sensors must be chosen which are reasonably robust. For operation on a remote tower, power is likely to be limiting so a low power drain is advantageous. For both tower operations and ship of opportunity operations reliable operation without servicing for extended periods is essential. It is also vital to be able to tell whether the data which are obtained are reliable. Thus it is useful to measure the same variable in more than one way. Because under high wind conditions damage to the sensors is inevitable, it is helpful to use commercially available components, preferably of moderate cost.

Some compromises may have to be made in attempting to satisfy all these requirements, particularly those of calibration stability and robustness, while still having sufficient sensitivity to measure the higher frequency contributions to the Reynolds fluxes. Working at high wind speeds has the advantage of improving the response if it is convection limited, e.g. temperature and some humidity sensors. Non-linear response of mechanical wind measuring equipment which occurs under light winds may also be ignored. Also, the nearly constant flux layer is thicker so one can work at greater heights. The sensors must be put fairly high to avoid waves and heavy spray and distortion of the air flow by the platform (e.g. a ship) in any case.

Ideally, one would like response to a normalized frequency $n = fZ/\overline{U}$ of 10 but 3 is adequate. Response 3 db down at n = 1 requires fairly small corrections (< 20%) and can be tolerated if the response is reasonably well known. The heights we have used are about 13 to 20 m for open ocean data with some intercomparison data taken at about 10 m. To get an indication of the response required, take $Z/\overline{U} \sim 1/2$ s, then n = 3 at f = 6 Hz. If the response occurs as a distance constant limitation as in a mechanical wind sensor, then the 3 db down frequency will be $\overline{U}/(2\pi D)$ where D is the distance constant. To get n = 3 requires $D = Z/6\pi$ or about 1/2 m for Z = 10 m and 1 m for Z = 20 m.

a) Temperature

To measure air temperature and its fluctuations we use glass-coated microbead thermistors (Victory Engineering Corp.). Their response is 3 db down at a few Hz at moderate wind speeds and improves with wind speed to about 30 Hz at 70 ms^{-1} (Miyake et al., 1970) and should be sufficient. (Better response can be achieved with resistance wire sensors but they are not as strong, require much greater amplification, which is more likely to cause problems, and are likely to be more subject to corrosion). The microbead is operated in a bridge circuit with a micropower operational amplifier as detector. By suitable choice of a resistor in series with the thermistor, the non-linearity of the bridge and thermistor can be balanced so that the output is linear within measurement error over a range of about 25 C°. The current through the bead is kept small enough that velocity sensitivity, because of variation in self-heating with flow speed, is negligible above 1 - 2 ms^{-1}.

A glass rod thermistor potted in soft epoxy is used to measure sea temperature a few metres below the surface when working on a tower. During our first major field operation which was on the beach at Sable Island, Nova Scotia, the sea temperature thermistor was put next to the microbead. Comparison of the two temperature signals indicated erroneous temperatures from the microbead after several days. We believe that the differences were caused by a saline moisture film across the bead and its leads. To avoid this problem and corrosion which eventually causes failure, we now insulate the leads right up to the glass coating using thinned-down transformer varnish (glyptol). The coating near the bead is done with a single hair brush under a microscope and tests have shown that complete insulation is achieved. We also added a sealed glass rod thermistor next to the microbead to provide a continuous check on it. With the coating the microbeads seem to be very reliable until they get broken, which happens very occasionally in spite of the protective cover we put them in. In our present field work on board the CCGS Quadra, one of the two ocean weather station PAPA ships, we have two microbeads to help ensure getting temperature fluctuation data.

The accuracy of our temperature measurements is about ± 0.2 C°; differences between sensors are accurate to ± 0.1 C° or better. The gains of the bridge amplifier were selected to give a full-scale range of 20 - 25 C° for the ± 5v input range of the recording system. The midpoint of the range is adjustable with a variable resistor in the other arm of the bridge. The recording system has 12-bit resolution so for temperature our resolution is ± 0.006 C°. The amplifiers were also designed to act as single-pole low-pass filters 3 db down at about 15 Hz, to reduce noise outside the frequency range of interest.

b) Humidity

In spite of trying several possibilities we have not found a humidity sensor with adequate frequency response which is suitable for unattended operation for reasonable periods of time. We initially rejected the α-Lyman humidiometer (Electromagnetic Research Corporation) because of relatively high power requirements (the latest model is much better in this respect), limited source tube life, and calibration drift due to window contamination and source tube aging. The α-Lyman humidiometer does have good frequency response (much better than any other humidity sensor we know of). It is limited by the path length between the tubes (about 1 cm) or more likely by the flushing of the protective cover one puts over it. Based on a local field test over land at moderate wind speed and comparison with the α-Lyman humidiometer, we found two other humidity sensors to try which appeared to have just adequate frequency response - an aluminum oxide sensor (Panametrics, Inc.) and a Brady array (Thunder Scientific Corp.). Both have low power requirements - a few mA. In local field trials of our system it still appeared that they would be possible to use, but on Sable Island where there is more salt in the air because of a much higher (and more oceanic) surface salinity we found the AlO_2 sensor to have rapid calibration drift and a limited lifetime. Unfortunately it is not suitable for use in a marine environment. The Brady array showed drift too, but it was not as severe. A second Brady array with a protective filter was added to replace the AlO_2 sensor in an attempt to provide a low-frequency calibration of the unfiltered Brady array. The calibration drift of the filtered array is much reduced but the analysis of the Sable Island data shows that the response of the unfiltered array is much poorer than we hoped. The poor response may be a salt contamination problem too. In any case, it appears that the Brady array is not suitable for measuring humidity fluctuations over the required range in an oceanic environment.

For our measurements on the CCGS Quadra (which occupies weather station PAPA half the time) we obtained a dew point system (Cambridge Systems Model 2000) to provide a low-frequency calibration of an α-Lyman humidiometer. It also provides another air temperature to check our other measurements. It seems to work for a month or so before salt contamination makes cleaning of the dew point mirror necessary. Unfortunately, serious contamination of the α-Lyman windows is quite rapid, within a very few days at best. We plan to use the dew point system and α-Lyman humidiometer during JASIN (Joint Air-Sea Interaction Experiment) in the North Atlantic in 1978 when we shall be on board and can do the necessary servicing in another attempt to measure and parameterize the moisture flux.

c) Velocity

There are a large variety of sensors to consider for this measurement. However, the conditions of being able to operate in rain, spray and perhaps snow or hail, and having good calibration stability, eliminate most of the possible sensors. We choose to base our velocity system on the GILL propeller-vane system (R.M. Young Co.) based on the experience of others in our Institute (e.g. Denman and Miyake, 1973) among many others. It is a mechanical system which has good calibration stability not only with a particular propeller but also from propeller to propeller, since the geometry is accurately maintained (even rather severe ablation of the propellers by rain, spray and hail does not affect the calibration measurably), which is simple and easy to service, which has very low power requirements (for the preamplifiers to give the tacogenerators the desired output range and to supply voltage to the direction potentiometer), and which works reliably for fairly long periods for moderate to strong winds. (For light winds the friction limits of a mechanical system become important but they are not of concern to us.) Furthermore, the sensitivity of the system is quite good. Quoted values of the distance constant are about a metre which is adequate if the observation height is large enough and if corrections are made when necessary. (A method of evaluating the response will be discussed in the next sub-section.)

These sensors have been used in a variety of ways. One is to use three propellers with their axes at right angles to give three components. Another is to use a propeller vane for the horizontal components and a propeller with a vertical axis for the vertical component. The problem with this second system is that the vertical component measurement is affected by non-linear response associated with friction and the driving of the tacogenerator for vertical components near zero. These problems occur for a velocity component less than about $\pm$ 1 ms^{-1}, although some correction can be made by adjusting the calibration coefficient.

To avoid this problem we modified the propeller-vane system by extending the vertical supporting shaft and adding a second propeller with an axis about 30° from the vertical. We have made this modification to some of the factory systems; we have also had the factory make a long vertical shaft system for us and added the attachment for the second propeller. The standard system of slip rings is already adequate with four slip rings with dual contacts (presumably for compatibility with a propeller bivane system, also manufactured); these are used in pairs for the two propellers. By using a 30° axis propeller we introduce some of the horizontal component (approximately ½) into this measurement. Thus this propeller always turns fairly rapidly, eliminating the region of stall and non-linear response for wind speeds larger than 4 - 5 ms^{-1}.

A photograph of the twin propeller-vane system is shown in Figure 1. The protective cover and radiation shield for the temperature (and AlO_2 or

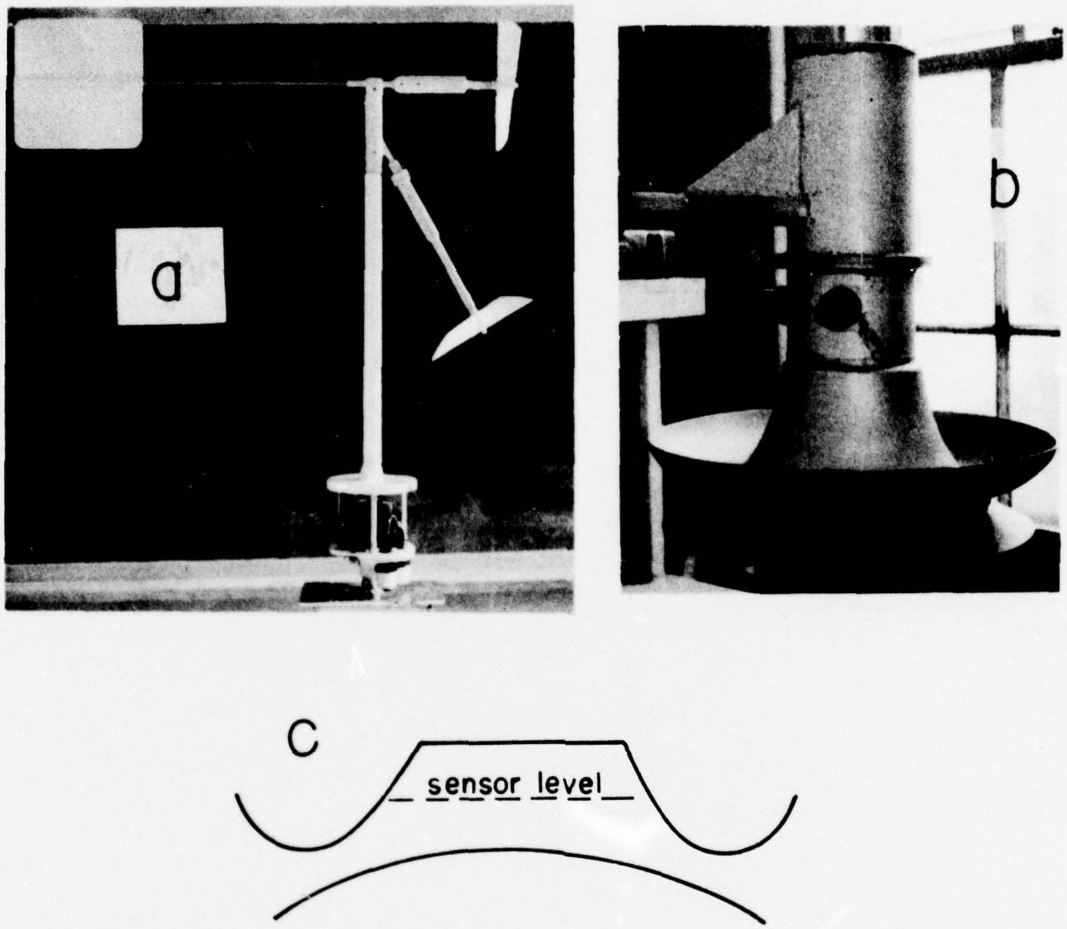

Fig. 1. a) Gill twin propeller-vane anemometer (propeller diameter 0.19 m).
b) Enclosure for temperature and humidity (AlO_2 and Brady) sensors.
c) Cross-section of flow path through the enclosure.

Brady humidity sensors when they were used) is also shown in Figure 1. The cylinder on top houses the temperature bridges and humidity preamplifier circuits. The anemometer preamplifier circuits are inside the housing at bottom of the anemometer. The preamplifiers have full-scale ranges (± 5v) of ± 180° for direction, of 50 ms^{-1} for the horizontal axis propeller and 35 ms^{-1} for the tilted propeller; they also act as single-pole filters 3 db down at 15 Hz to reduce high frequency noise. The resolution is 1/4096 of these values or 0.09°, 0.012 ms^{-1} and 0.009 ms^{-1}, respectively.

These propellers do not follow a cosine law exactly, but compensation for the non-cosine behaviour can and must be made. A detailed discussion is given in the Appendix along with a detailed error analysis. Correction for the non-cosine response is necessary at both first (important) and second order (probably not essential - see Appendix). The propeller with its axis nearly horizontal seems to follow cosine response from existing measurements for $|\delta| \lesssim 5 - 10°$ and measures

$$v_1 = Q\cos\delta + w\sin\delta$$

where δ is the small tilt angle when the instrument is not level, with δ taken positive for a tilt down into the wind (see Fig. A.1) and Q is the horizontal wind component $(U^2 + v^2)^{\frac{1}{2}}$. The propeller with its axis at 60° nominal from the axis of the v_1 propeller measures

$$v_2 = [Q\cos(\alpha+\delta) + w\sin(\alpha+\delta)][1 - 0.328(\delta - \tan^{-1}(w/Q))]$$

where α is the angle between the propeller axes. The correction factor $1 - 0.328(\delta - \tan^{-1}(w/Q))$ comes from the non-cosine response. There is some uncertainty in the 0.328 coefficient (the value for $\alpha = 60°$) and its variation with measured values of α should be and is taken into account. The deviation from cosine response for the measured α (here taken to be 60°) and $\delta = 0$ and $w = 0$ is included in the calibration for v_2 (see Appendix). The method of analysis is to measure $\overline{v}_1$ and $\overline{v}_2$ (— indicates averages over about 1 hour) and to take $v_2 - (\overline{v}_2/\overline{v}_1)v_1 = -c = aw^2 + bw$ and solve the quadratic for w. The effect of the aw^2 term is small and nearly negligible as shown in the Appendix but is retained. The various errors in calculating w, Q (and hence $U = (Q^2 - v^2)^{\frac{1}{2}}$) are discussed in the Appendix. It is important to remember that any errors in w and δ calculated from $\overline{v}_2/\overline{v}_1$ will propagate into the calculated q and hence u. A summary of the possible errors based on the analysis in the Appendix is given in Table 1. Careful measurement of α is clearly essential. Good D.C. stability of the amplifiers and offsets (applied to make the outputs $\simeq$ -5v for no wind) are also important and we have been very careful about these points using the best low temperature coefficient zener diodes for reference voltages. The presence of some Q in the tilted propeller also helps to provide a check of proper operation since low pass filtered v_1 and v_2 signals should and do look essentially the same. There is no double check on the wind direction but it is not essential to measure the Reynolds stress (see Appendix) except to indicate when we are in the wake of some part of the platform, but such effects are also evident from the v_1 and v_2 measurements. In any case we have only had to replace one direction potentiometer when a check in the laboratory showed it was not working well over its full range.

d) System interconnections

This problem is often not discussed but in fact is not trivial. The use of so-called weather-proof connectors can lead to grief - often considerable. In our system we use underwater connectors (Mecca connectors made by Teledyne Corp.) which are of reasonable cost; other similar connectors are also available. In our experience, such connectors are essential since the recording package part of the system goes underwater at times (during our work on Sable Island and on the Bedford Institute stable tower). Thus, we recommend the use of underwater connectors in all parts of the system exposed to the marine environment.

e) Sensor response

To get the spectral level measurements to make dissipation estimates requires a measurement in the -5/3 range. Because of the response limits of the sensors we must work at the low-frequency end of the range to avoid having to make large corrections for the response limits. We chose to use three frequency bands centered at 0.4, 0.8 and 1.6 Hz as a compromise. Having three bands allows a check on the -5/3 slope with the observations; it also allows a band to be dropped if its n value becomes too small (e.g. the 0.4 Hz band when $Z/\overline{U} < \frac{1}{2}$ s) or when the response correction becomes rather large (e.g. the 1.6 Hz band for a D of 1 m and winds less than 10 ms^{-1}).

Table 1. Summary of possible errors

Cause	Effect on $\|\overline{uw}\|$	Effect on C_D	Comments
α error of ± 1°	± 5 %	± 5 %	We believe α error is actually within ± ½ ° and effect ± 2 - 3 %.
Offset error	± 2 % at 5 ms^{-1} ± 1 % at 10 ms^{-1}	± 3 % at 5 ms^{-1} ± 2 % at 10 ms^{-1}	Actually, offset errors partly cancel rather than add and are about ½ these values.*
Calibration error of ± 2 %	± 4 %	± 1%	
Errors in $\beta'(\theta)$	± 3 %	± 3 %	
Fluctuations in δ	Negligible	Negligible	
Non-cosine response of v_1 propeller	± 1 % for $\delta = 0$ ± 10 % for $\delta = \pm 10$	± 1 % for $\delta = 0$ ± 10 % for $\delta = \pm 10$	For $\|\delta\| < 2 - 3°$ similar to $\delta = 0$. For $\|\delta\| = 5$ probably within ± 5 %.

If everything goes wrong including all the data having δ equal either + or - 5°, $|\overline{uw}|$ may be in error by about ± 18% and C_D by ± 16% but with δ varying and some errors perhaps tending to cancel rather than add, we may hope to get average C_D's within ± 10% which is fairly comparable to any other system. For dissipation estimates only calibration and offset instrument errors are important. For a +2% calibration error u_*^2 is in error by 2.7% and C_D by -1.3%. At 5 ms^{-1} the offset error leads to a 0.3% error in u_*^2 and a 1.3% error in C_D. Most of the uncertainty in this method comes from uncertainties in the values of κ, K' and Z and the assumptions made to use it.

*Note that the quoted values require d.c. stability of 1/2000 of full scale (50 ms^{-1} in our case) for 2 - 3% error at 1/10 of full scale (5 ms^{-1} in our case).

If we assume that the sensors behave as simple RC filters, then the spectral values from two different bands in the -5/3 range can be used to determine their response characteristics in turbulence. We can find the value of 3 db down frequency, fo, that gives the same value of ε or N_γ from the two bands, over a range of wind speeds. If the response can be represented by a distance constant ($\bar{U} = 2\pi\, fo\, D$), then a plot of $\bar{U}$ vs. the required $2\pi\, fo$ should be a straight line through the origin. Figure 2 shows such a plot based on hourly averages of the 0.8 Hz and 1.6 Hz filter data from one of the Gill v_1 propellers on the Bedford Institute stable platform. Much of the scatter is probably due to statistical variations from the -5/3 slope. This scatter increases at higher values of $\bar{U}$ because the corrections become relatively insensitive to fo when fo is large compared to the center frequencies, and therefore it takes a larger change in fo to compensate for the same relative difference in the calculated ε's. The corrections are also non-linear which skews the scatter to high values of 2π fo. The plots suggest that the apparent distance constant decreases with wind speed. Data from all three filters have been used to give the solid line, $D = .56\ \bar{U}/(\bar{U} - 1)$. A fit through the origin, to 12 ms^{-1}, gives a distance constant for this anemometer of 0.63 m. Finding a distance constant for the v_2 propeller is more complicated because we essentially measure a combination of U and w. One must use observed ratios of ϕ_w/ϕ_u and ϕ_{uw}/ϕ_u to estimate the departure of the spectral slope from -5/3. The value calculated for the v_2 propeller is .76 m of air flow in the horizontal. This is about 20% larger than the v_1 value, perhaps a reflection of the deviation from cosine response which is also about 20% for $\alpha = 60°$.

We have found similar values for other instruments, however one of these also gave values of 1.0 m for v_1 and 1.2 m for v_2 for some early data. This was a bit puzzling, but it turned out that the earlier propellers were nearly twice as heavy as those purchased more recently. All the propellers we have used are the 7½" diameter two-bladed type which have the greatest strength. The quoted distance constant is 0.8 ms^{-1} so the observed performance of the lighter propellers in turbulence is somewhat better than claimed. As noted by Hicks (1972) the initial response is a little better than expected from a single-pole filter behaviour and perhaps this behaviour explains why the observed distance constant is better than that predicted from the length required to reach $(1 - e^{-1})$ of full speed from a zero start.

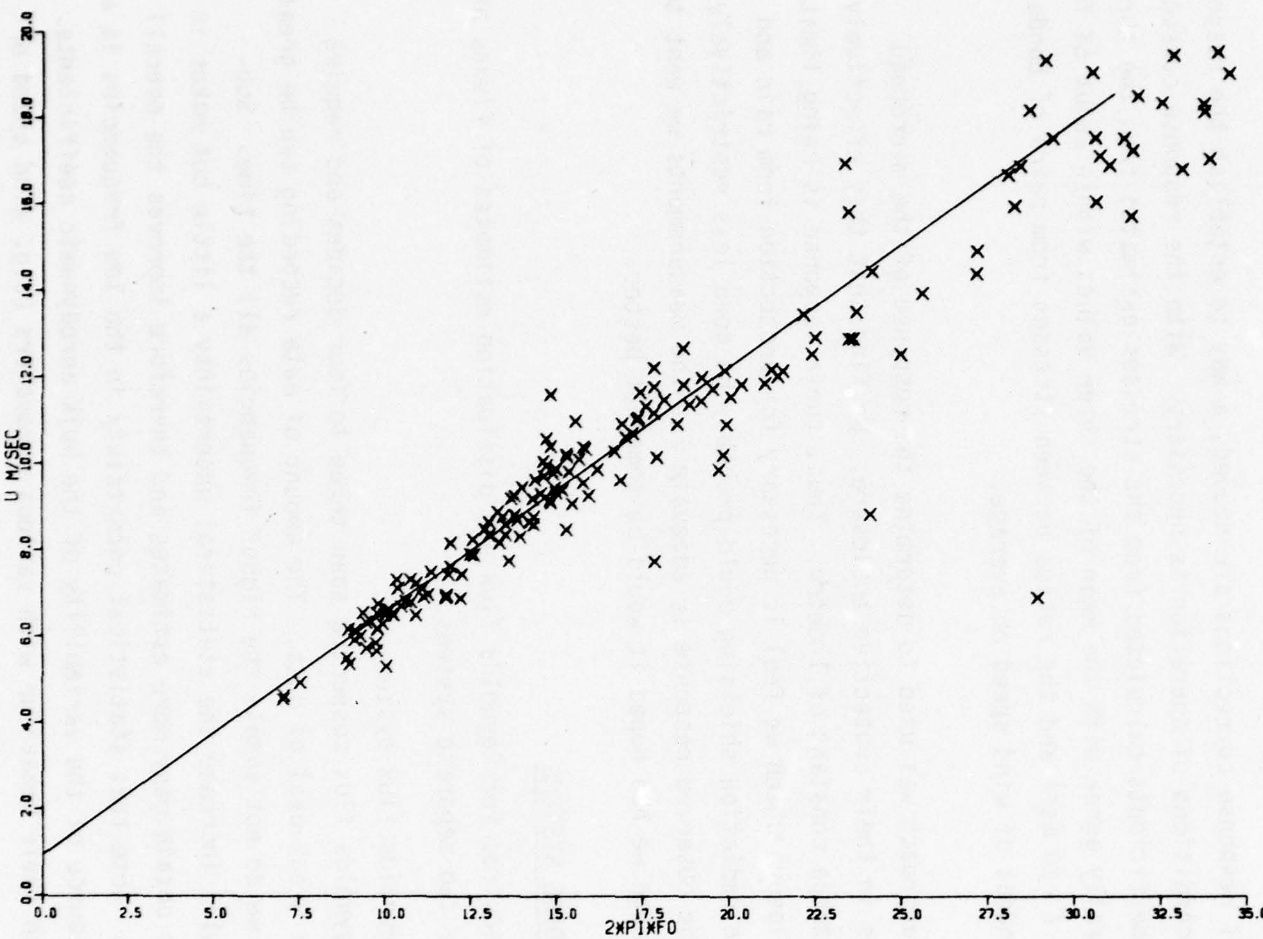

Fig. 2. Plot of $\bar{U}$ against the value of 2π fo required to make ε's calculated from the 0.8 and 1.6 Hz band pass filters equal. The line is a fit to data from all three filters and gives $D = 0.56\ \bar{U}/(\bar{U} - 1)$ m.

It is no longer possible to obtain the type of propeller we have been using - a new four-bladed version with slightly different calibration is now being made. We have not established its response as yet, but judging from the weight it should be similar to the better old type of propeller.

Clearly, if response corrections are needed, a way to establish the response under the conditions of operation is necessary. With the response corrections the drag coefficients calculated from the stresses estimated from the three bands generally agree with the mean of the three values within about 5% for winds from 6 - 20 ms^{-1} and the ratios between stresses from pairs of bands are independent of wind speed on average.

A similar approach was used to determine the response of the microbead thermistors in their protective enclosure. We find that they effectively have a distance constant of 1 metre. Thus, their response is being limited by the enclosure which we feel is necessary for protection from rain and spray - the radiation shielding could probably be done less restrictively. However, the observed response is adequate for the measurements we want to make, although we had hoped it would be somewhat better.

IV. RECORDING SYSTEMS

The data required for Reynolds flux and dissipation estimates of fluxes are recorded by two separate systems.

a) Reynolds flux system

The Reynolds flux cospectra span three to four decades and require recording a great deal of data. The amount of data recording can be greatly reduced if we do not sample the higher frequencies all the time. Sub-sampling will increase the statistical uncertainty a little but makes it possible to obtain many more estimates and therefore improves the overall statistics. Note that statistical uncertainty in the low frequencies is an important source of the variability of the bulk aerodynamic coefficients. To establish their behaviour with various parameters (e.g. wind speed or stability) requires a large number of estimates. For remote operation, sub-sampling is required because of the data storage limitations of low power recording systems.

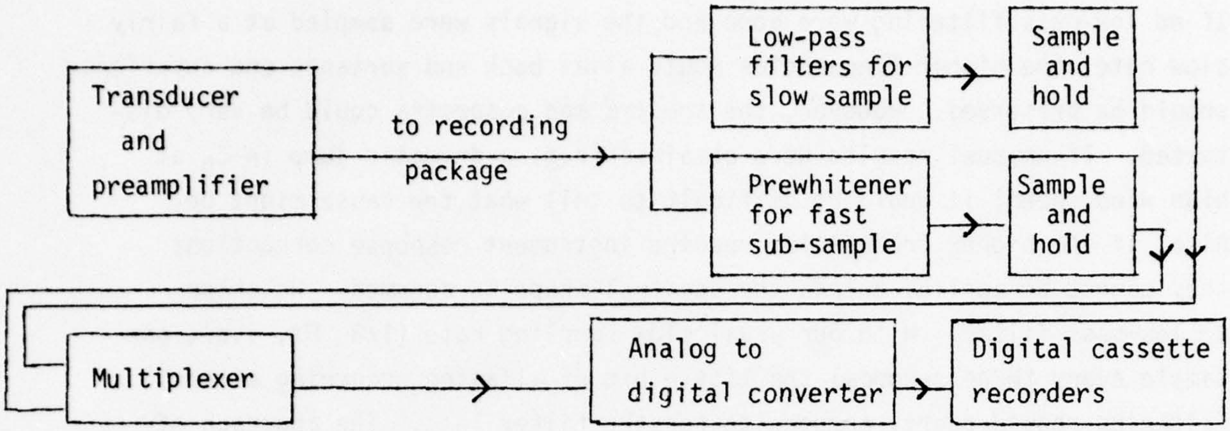

Fig. 3. Block diagram of data flow in the Reynolds flux recording package.

A block diagram of the data flow in this recording system is shown in Fig. 3. Up to six channels may be sampled. Three of these are from the twin propeller vane anemometer; the other three are scalar signals - the microbead thermistor and two of the various humidity sensors we have tried. During our present work on the station P weathership CGSS Quadra, we have used two microbeads. In our planned work during JASIN we shall record a microbead, α-Lyman humidity and dew point temperature. By recording these two humidity signals we can calibrate the α-Lyman against the dew point at higher frequencies than we can with the dissipation system.

In the Reynolds flux system each signal from a transducer preamplifier goes to a pair of circuits: one is a low-pass filter with a one-second time constant (3 db down at 0.16 Hz); the other is a prewhitening circuit to emphasize the higher frequencies. The low-pass filter is an RC filter with a micropower operational amplifier follower on its output (gain 1.000). This signal is used for a slow sampling rate sample. The prewhitening circuit acts like a time differentiator at low frequencies, reaches maximum response at 1.5 Hz and then rolls off like an RC low-pass filter at higher frequencies. It also uses a micropower operational amplifier as the active element. This signal is used for a fast sampling rate sample.

If no low-pass filtering were done and the signals were sampled at a fairly slow rate, the higher frequencies would alias back and variance and covariance should be preserved. However, the spectra and cospectra could be very distorted. If unusual results were obtained (e.g. a dramatic jump in C_D at high wind speed) it would be difficult to tell what the cause might be. Also, if the higher frequencies require instrument response corrections they cannot be applied unless the spectral shape is assumed. We chose to low-pass filter. With our usual slow sampling rate (1/3 Hz, i.e., one sample every three seconds) the little bit of aliasing occurring after filtering should nearly compensate for the filter loss. The approach of allowing full aliasing and using the high frequency subsampling to tell what aliasing is occurring and hence what instrument corrections are needed should work but is somewhat more complicated.

By using the prewhitening circuit we eliminate any spectral distortion due to frequencies below those sampled (which, because of the greater amplitudes at low frequencies, have an effect similar to a large trend). The signal level is also increased, which keeps the digitization noise at a very low level. The gain is chosen so that the mean square output is about 1/50 of full scale for the largest expected signals allowing fairly large peak factors and considerable error in our estimates of the required gain (for a sine wave the peak-to-peak value would be 1/5 of full scale). In practice overloading has not occurred so far in our observations. Our fast sampling rate is 3 Hz (limited by the digital recorders). By allowing the response to be flat at 1.5 Hz (the Nyquist frequency) we do allow the high frequencies which we cannot sample to alias back so that we do not lose their contribution. Of course the frequencies above 1.5 Hz are somewhat undercorrected for instrument response. Except for ϕ_w, the aliasing effects are small. Undercorrection for instrument response should be negligible except perhaps for σ_w. Since our primary concern is the fluxes these limitations are not serious.

Sample and hold circuits are used to avoid the need to correct for time skewness in the sampling. The multiplexer allows the A/D (analog-to-digital converter) to sample the fast or slow channels in sequence (up to a maximum of 6).

The A/D converter is a 12-bit low power unit (Analog Devices). With 12-bit accuracy the signal to noise ratio is potentially about 83 db. In our experience, digitization noise is the limiting factor; with no signal (no propellers and dummy resistors for temperature and humidity sensors) the change in the A/D value is at most ± 1 bit. Now the rms fluctuations for wind are about 1/10 of the mean, or about 20 db down at full scale (50 ms^{-1}), and 40 db down at 1/10 full scale (5 ms^{-1}). For the slow samples the variation over the frequency range sampled is perhaps another 20 db so even the lowest spectral values have about 20 db signal-to-noise ratio. For the fast samples the signal is about 17 db below maximum at 50 ms^{-1} and 44 db at 5 ms^{-1}. The spectra are nearly flat so there should be no problem. For temperature, the full scale is about 20 C°; with an air-sea temperature difference of 1° the rms fluctuations are about 0.1°, or about 46 db down for the slow samples and 38 db down for the fast samples if $U = 5$ ms^{-1}.

In the scheme we have usually employed, the prewhitened signals are sampled at 3 Hz for 128 samples (42.7 sec) and then the low-pass filtered signals are sampled at 1/3 Hz for 256 samples (12.8 minutes). This sequence is repeated four times to form one data group to give one Reynolds flux estimate (over a period of 54 minutes). A time word (the number of 0.1-hour intervals since start-up) is written at the end of each group. As it is also 12 bits it folds over after 17 days, but the folds are easy to allow for. A check on the contributions from lower frequencies can also be made from the means over the 12.8 minute slow samples. The fast sample rate is fixed but the slow sample rate may be varied from 1/3 sec to 33 sec in 1/3-sec increments. The number of samples of each type may be varied from 2^4 (16) to 2^{13} (8192) and the number of fast and slow sample pairs in a group from 1 to 9. The time interval between collecting groups may be varied from 0.1 to 99.9 hours in 0.1-hour increments. Usually we have used 3.0-hour intervals.

The digital cassette recorders we have used are those made by Memodyne. Their specifications allow them to be used at up to 100 steps (and bits) per second. To get our 3 Hz sample rate we run a pair of recorders at 150 steps/sec to get three channels per recorder. At this stepping rate they are somewhat sensitive and one must pretest the cassettes to be sure they will work well in a particular machine. In retrospect, it might have been better either to have accepted a 2 Hz sampling rate and a little more aliasing distortion or to have run three recorders with two channels each. We record the 12-bit words as a 2-bit gap (no flux changes) and the 12-bit word. A mark character (2-bit gap + 1 bit) separates each scan (sample) of three channels. These choices were made to avoid losing track of the words even if a bit were lost. In practice, we have had more trouble with gap recognition than losing bits and could probably have omitted the gaps completely, but we didn't know what the limits were when we started.

Originally we started with standard digital cassettes (equivalent to a C60 audio cassette in length). Later we switched to C90 type cassettes (Information Terminals) to increase the record length. C120 cassettes have also been used by others but with our high stepping rate might not be satisfactory - we have not made a systematic check on such cassettes.

With a C60 cassette we have room for 30 groups of four each of 128 fast and 256 slow scans; with the C90 cassettes we get 44 such groups on one tape. With a 3-hour interval, this allows 5.5 days of data on a C90 cassette. To extend the data length further we use three pairs of recorders which allows 16.5 days of recording.

Even this length is somewhat short. More recorders, a different type of recorder or a longer interval between recordings provide alternatives. Sampling at greater than 3-hour intervals is not attractive since one would get only a very small number of samples during a particular high-wind speed event. (Sampling more often is probably unnecessary as more frequent samples are not completely statistically independent.) Recognition of the fact that many of the samples will not be of interest allows one to extend the total sampling length. Low winds (< 5 ms^{-1}) are of little interest. Even winds < 10 ms^{-1} soon become of little interest. A circuit was added to average the wind speed over 0.1-hour (six minute) intervals, the basic interval rate of the recording system. When a record was to be taken, it would not be allowed if the mean speed was below a set limit in the preceding six minutes. The settings were 0 - 9, allowing recordings for all winds at setting 0 and 6 to 22 ms^{-1} in 2 ms^{-1}-increments for settings 1 to 9. Thus, with a setting of 3 (10 ms^{-1} lower limit) as usually used on the Bedford stable platform experiment, records would be taken only about 1/3 of the time on average, giving recordings for up to about 45 days. With an intended service interval of 30 days, this scheme seemed to provide sufficient length to allow for bad weather delaying servicing and proved adequate in practice.

The prewhitened signals must be corrected for instrument response. In the case of the v_1 and v_2 signals these corrections must be applied before u and w can be calculated because of the need for a non-linear correction (see Appendix). The v_1 and v_2 signals are Fourier transformed, corrected for the circuit and instrument response and inverse transformed using the first slow sample value following the fast sample to give the offset needed for v_1 in calculating w. u and w are then calculated and Fourier transformed. To calculate $\overline{uw}$, other covariances involving w and spectra, the slow sample values are used for frequencies up to their Nyquist frequency (1/6 Hz) and the fast sample spectral and cospectral values at frequencies above 1/6 Hz are used for the high frequencies. Originally we planned to 'correct' the fast sample values by comparing spectral and cospectral values in the overlap region 1/43 Hz to 1/6 Hz, but because of statistical variation in the lower frequencies of the fast sample results this procedure seems to be less satisfactory than just using the observed fast sample values for frequencies above 1/6 Hz. More sampling to reduce the variations above 1/6 Hz should be done if possible, although we couldn't during the Bedford stable platform experiments.

b) Dissipation system

This package provides continuous recording of the variables, their low-frequency variations, and spectral levels from which dissipation estimates may be made. The data flow for a channel for which both low-frequency and spectral band information is desired is shown in Figure 4.

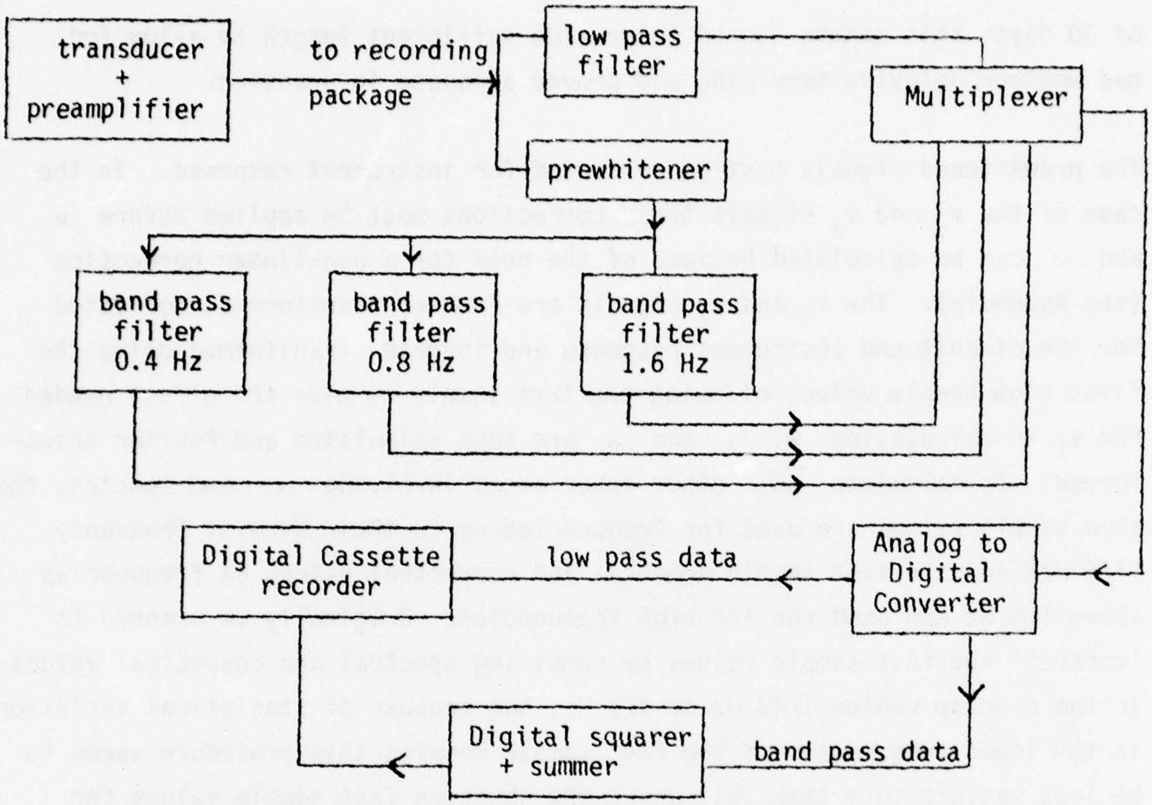

Fig. 4 Data flow in the dissipation recording system.

Spectral band data are obtained for both the v_1 and v_2 propellers. The v_2 propeller data provide a check and are collected to allow dissipation estimates to be made if the v_1 channel fails before the v_2 channel. Such estimates being a mixture of ϕ_u, ϕ_w and ϕ_{uw} would have more uncertainty; however, so far, when we have data, both signals are present and only the v_1 band pass values are used. Spectral band data are also collected from the microbead and have been attempted (unfortunately with little success) from the various humidity sensors. Hopefully, we shall get some useful data with the α-Lyman system during JASIN.

The low pass filters are 25-second single-pole RC circuits followed by a micropower operational amplifier in a follower mode (gain 1.000). Channels for which spectral data are not required have the low-pass filter treatment only, e.g. sea temperature, wind direction, filtered Brady array (when used), air temperature from the rod thermistor, air temperature from the dew point system (when used) and dew point temperature (when used). A maximum of 20 low-pass filter channels can be recorded but up to now we have only recorded nine data channels plus a zero reference to check for drift. In our earlier work the zero reference was a grounded low-pass filter circuit (no drift within the A/D resolution was experienced). When we added channels and used all of the nine low-pass filter circuits initially installed the zero reference became a grounded multiplexer channel.

The prewhitener circuit acts as a differentiator at low frequencies, reaches peak gain at about 10 - 15 Hz and rolls off as a single-pole RC filter at higher frequencies. A micropower operational amplifier is the active element. It makes the input spectrum to the band pass filters nearly white. For a -5/3 input spectrum the output spectrum is +1/3 in the band pass filter range. The gain was chosen to make the mean square output about 1/50 of full scale for maximum input (e.g. 50 ms^{-1} for wind, ΔT = 5 C° with $\bar{U}$ = 25 ms^{-1} for temperature). The band pass filters are an RC double-pole high-pass stage followed by a double-pole low-pass stage using a dual micropower operational amplifier as the active element. Care was taken to make the final DC output very small and stable. Again, the gains were chosen assuming a -5/3 original input spectrum to make the mean square output 1/50 full scale at maximum input to allow fairly large peak factors and leave leeway for errors in the design criteria (for a sine wave the peak-to-peak value would be 1/5 of full scale).

Over most of the interval between recordings each band pass channel is sampled at 20 Hz, the output digitally squared and summed. (In a second package using a microprocessor, the sample rate is 10 Hz because squaring by the microprocessor is slower than the hard-wired version of the original package). Analog squaring of the signals was considered briefly, but was quickly discarded as having inadequate dynamic range. The accurate range of analog squaring is about 20 db or so. However, for a wind velocity signal with C_D, σ_u/u_*, and hence $\sigma_u/\bar{U}$ independent of $\bar{U}$, the output power of a fixed frequency band pass filter is proportional to $\bar{U}^{8/3}$. For a change in $\bar{U}$ from 5 to 50 ms^{-1} the power output changes by about 500, or 27 db. Since we must allow about 20 db from full scale for peaking and possible underestimates of C_D at high $\bar{U}$, analog squaring is much too inaccurate. For scalars the power output is proportional to $\bar{U}^{2/3}(\Delta\gamma)^2$

In calculating the squares, one has effectively an 11-bit number since the sign does not matter. We decided to retain the high order 20 bits of the square, the lower 2 bits probably being mainly noise. These 20 bits were accumulated in a 32-bit register. With 4096 squares (∿ 205 seconds), full-scale readings would fill the 32-bit register but since the mean square value should be about 1/50 of full scale the register will have zeros in the first 5 or 6 bits in fact.

To record the values in the registers a floating point format was used. Shifting along the register for up to 15 shifts was used until a one bit was found. The number of shifts was recorded in the first 4 bits and the 8 bits in the register after shifting was recorded as the last 8 bits.

This scheme does not use the full dynamic range of the system, in fact, and also does not give a full 12 bits of information except for small values. If there are less than 15 shifts the first bit in the remaining eight is always a one. However, the scheme used does allow adequate dynamic range and ensures that non-zero bits are signal, not noise. A shift of up to 25 places (requiring a 5-bit exponent) could be used if more dynamic range is needed, but the resolution of the mantissa would only be 1/64 unless the first bit was dropped except when 25 shifts occurred. The dynamic range allowed is 2^{24} or 72 db, less than the noise level of 83 db which will be further reduced by summing many values.

Suppose $\overline{U}$ = 2.5 ms^{-1} or 1/20 of full scale; then the power output of a band pass filter of a velocity signal is about $(20)^{-8/3}$, or 35 db down from the value expected at 50 ms^{-1} which is 17 db below full scale, for a sum of 4096 squares; the 52 db down total is still 20 db above the zero value. If a larger or smaller number of squares are summed, there is still plenty of range. For example, for 1024 iterations the signals at $\overline{U}$ = 2.5 ms^{-1} are still 14 db above the zero value, i.e. the resolution is still 1/25 of the reading. For temperature with $\overline{U}$ = 1.25 ms^{-1} and ΔT = 0.25 C° (both 1/20 of design) one is also 20 db above the minimum value, for a sum of 4096 squares. Thus, the scheme we have used is adequate since the minimum values used as examples are below those used in practice, and when one gets near zero values one is sure the fluxes are small (as confirmed by the small directly recorded values of $\overline{U}$ and ΔT). For very light winds (< 1 - 2 ms^{-1}) brush noise from the tacogenerators may give non-zero band pass outputs for v_1 and v_2, but these are obvious and brush noise is at too high a frequency to cause measurable effects at wind speeds of interest.

The low-pass filter outputs and the sums of squares of band pass filter outputs (up to 20 channels) are recorded at intervals. One to 20 of each type are selectable but 9 low-pass and 15 band pass filter channels plus a zero reference for each are the maximum used so far. After each scan, a 4-bit identification word and the lower order 8 bits of the scan count are recorded. The high order 12 bits of the scan count is also recorded after each block of scans (maximum number before folding is 2^{20}). The number of scans per block may be selected from 1 to 99 and the number of blocks per tape from 1 to 999.

The sample interval may be varied from about 6 sec (minimum to allow recording and bookkeeping) to 999 sec. The number of iterations (number of squares in the sum) is chosen to use most of the time between recordings. Maximum allowed is 9999 at 20 Hz (8.3 minutes) in the first package and 4090 at 10 Hz (6.8 minutes) in the second package built. Our basic design time interval was 4 minutes, allowing up to 4600 squares to be summed (or 2300 in the microprocessor controlled package). We have used 2- or 4-minute intervals in earlier experiments. Presently on the weathership program, we are using 5-minute intervals allowing 28 days of data on one tape. We use two recorders in sequence, allowing 56 days total which is a bit longer than one patrol of 48 days including time to and from station.

c) Circuit response measurements

The detailed response of many circuits must be measured in the system - in particular, the 6 prewhitener circuits in the Reynolds flux package and the 15 band pass filters, including the effect of the preceding prewhiteners, in the dissipation package. Measuring the response by analog means is both tedious and awkward because of the frequencies involved. A good chart recorder is about the only means and amplitude ratio accuracy of about 2% is about the best one can do. This method was used at a few points to check the digital method actually used.

The method used was to generate a white spectrum (sum of sine waves of equal amplitude) over the frequency range of interest on our PDP-12 computer and generate an analog signal using a D/A converter. The D/A holds the output until updated and thus has a staircase character, but by going to somewhat higher frequency than finally needed and low-pass filtering, a white spectrum with a smooth roll-off is produced. This spectrum is passed through the circuits and both the input and output are digitized on the PDP-12. Fast Fourier transforms are done on the UBC Computing Centre IBM 370 from which the transfer function including phase may be computed accurately. As the PDP-12 has a 10-bit A/D the dynamic range is 60 - 70 db which is adequate. Originally we tried generating white noise using random numbers, but the white spectrum with the generation frequencies matched to the sampled frequencies gives more coherence between input and output when the transfer function is small.

For the prewhitening circuits of the Reynolds flux package the transfer function is quite small at low frequencies but needs to be known accurately. A straight line was fitted in this region to smooth out the small random errors. For the band pass filters of the dissipation package such measures are not needed. However, because the bandwidth is fairly large it is necessary to allow for the spectral shape of the actual turbulence data. In calculating the relation between the input power and the final output, a -5/3 spectrum was assumed.

d) Power requirements.

Digital recording offers great advantages for remote operation in terms of wide dynamic range and low power. (Although the low power digital tape units require some compromise, e.g. subsampling the higher frequencies in the Reynolds flux package.) The overall power requirement for the transducers, the flux package and the dissipation package is about 50 mA at 36 v nominal (28 - 40 v range). The 36 v was chosen to be compatible with the power supply on the Bedford Institute of Oceanography stable platform; the system could be adapted to run on 24 v fairly easily to reduce the number of batteries required. Negative supply voltages needed for the analog circuits are generated internally. Substitution of the microprocessor dissipation package increases the current drain to about 100 mA, so the greater flexibility of using a microprocessor does require extra power.

V. IN-FIELD READER

A serious problem with all digital recording instruments is how to check them for proper operation in the field. Monitoring connectors on the recording packages were included so the preamplified transducer signals could be checked. One can also see if the tape recorders are advancing correctly but these checks are insufficient and it is not satisfactory to wait until the cassette can be translated to standard 9-track tape on our PDP-12 system in the laboratory. Thus, to provide a check in the field, a reader unit was constructed to decode the output from a Memodyne reader unit and provide signals for a six-channel chart recorder (a Brush 260 in our case).

For the dissipation package records the unit can be set to start on any channel and decode six sequential channels. A 10-bit D/A was used because a 12-bit unit was not readily available when the unit was built, but it is adequate for chart monitoring. The low-pass channels are put out directly. For the band pass channels the first 4 bits (the exponent) are inverted so that increasing power gives increasing output, the first bit of the remaining 8 is dropped (unless the exponent indicates 15 shifts) and the others are shifted. The output, then, is approximately $\log_2$ (of band pass output). Actually, it is a set of sixteen linear segments approximating a logarithmic curve. The in-field reader proved invaluable in checking for proper operation and gives an excellent indication of it. For example, when working properly the v_1 and v_2 low-pass signals should and do look very similar, the microbead and rod thermistor air temperatures' low-pass signals look similar. Likewise, the band pass outputs for a given transducer all follow one another. The reader will also put out the three data channels plus time channel from a Reynolds flux package tape.

VI. FIELD MEASUREMENTS AND SOME PRELIMINARY RESULTS

After local field testing our first field expedition with the equipment was to Sable Island, Nova Scotia, for an intercomparison experiment with the air-sea interaction group of the Bedford Institute of Oceanography in September and October 1975. Our preamplified transducer signals were also recorded on the BIO recording system and initial analysis of these records was performed at BIO for comparison with their results.

The shortcomings of the humidity sensors we were trying, which this experiment revealed, have already been mentioned in section III b. A need to improve our temperature measurements was also indicated, as discussed in section III a.

The results of this experiment were written up jointly as a BIO technical report (Smith, et al. 1976). The main results are that all the wind sensors (Sonic and thrust from BIO and Gill from IOUBC) gave comparable results (our GILL anemometer system required response corrections, as expected) and that the indicated values of C_D are similar to those reported by Smith and Banke (1975) mainly based on offshore tower data. Detailed response corrections to the GILL were not made but were allowed for by comparison with the BIO results and seemed reasonable if the distance constant were about 1 m. At that time we had not established the exact distance constants as discussed in section III e. However, the covariances at a given height come from a fixed range of length scales so if the response limit occurs as a distance constant, the correction is independent of $\bar{U}$. Our own analysis of these results is still in progress but it appears that with detailed corrections both Reynolds flux and dissipation estimates give similar results to those presented in Smith et al. (1976).

The next field experiment was also conducted with the air-sea group at BIO on their stable platform - about 10 miles offshore of Halifax, Nova Scotia. Again, analysis on their system gives comparable results with smaller response corrections to the GILL system indicated (probably because of the greater height and also because of the better-response newer propellers). Our analysis is giving similar results with C_D values generally agreeing with the Smith and Banke (1975) curve showing an apparently fairly slow linear increase of C_D with $\bar{U}$. Measurements were attempted from September 1976 through April 1977 and a great deal of data were obtained. We are particularly pleased with the amount of data obtained above 15 ms^{-1}. Table 2 shows the number of Reynolds flux estimates and number of hours of dissipation data obtained for unlimited fetch conditions ($\frac{1}{2}$ - 1 hour of dissipation data is sufficient for a flux estimate). There are also data for limited fetch which we shall examine. We also plan to look at the time variation of C_D with storm front passages, 13 of which we have identified.

Table 2. Unlimited fetch data from the Bedford Institute stable platform.

wind speed (ms^{-1})	6 - 8	9 - 11	12 - 14	15 - 17	18 - 20
# of Re flux records	67	79	82	32	13
# of hrs of diss. data	165	175	77	53	33

Our next field experiment started in July 1977 with our system being installed on board CCGS Quadra, one of the two ships which occupy ocean weather station PAPA. The first patrol was during MILE (Mixed layer experiment) and in spite of unintended shut-down problems caused by power line transients, a good deal of data were obtained thanks to the efforts of Dr M. Miyake and his staff who were on board running another program. A good deal of work had to be done to reduce radio transmission interference which was increased by adding the α-Lyman and dew point systems and their cables. After the second patrol the dew point and α-Lyman systems were removed as it became obvious that few useful data were being obtained by them. On the third patrol which was recently completed, the system ran throughout although both microbeads were broken after a few days. The last patrol on which we shall operate starts in late March 1978 and ends in early May. Quite a few observations for winds up to 20 ms^{-1} have been obtained with a few occasions of winds to 25 ms^{-1}. An exact list including corrections for ship's velocity has not yet been compiled.

Our next field operation (and probably the last, at least for some time) will be on the Meteor during JASIN. Here, one of us (WGL) will be on board and another attempt can be made to get moisture flux measurements using the α-Lyman humidiometer for fluctuations with the dew point system to provide *in situ* calibration.

ACKNOWLEDGMENTS

We wish to thank the many people who contributed to the design and construction of this system. Dr M. Miyake first brought our attention to the good qualities of the GILL propeller anemometers and their use by him and his students led to our twin propeller design. Mr E. Meyer was responsible for the electronics design and much of its construction. Mr D. English and Mr H. Heckl assisted with the mechanical design and construction. Mr P. Merchant also assisted with construction work. Mr D. Fissel calculated the gains required for the prewhitener and band pass circuits. Mr B. Walker developed the PDP-12 computer method of measuring circuit response.

We also wish to express our thanks to Professor R.W. Burling for many helpful suggestions and to Dr S.D. Smith and his air-sea interaction group at the Bedford Institute for making it possible to do the intercomparison experiments with them. Finally, our thanks to Miss D. Blackwell for typing the manuscript.

Support for the work was provided by the U.S. Office of Naval Research (Contracts N 00014-66- C-0047 and N 00014-76-C-0446 under Project 083-207) and the National Research Council of Canada (grant A8301).

REFERENCES

Burling, R.W. and R.W. Stewart, 1967: Ocean-Atmosphere Interaction (Microprocesses). In *Encyclopedia of Oceanography*; R. Fairbridge, ed., Rheinholdt, New York, p. 571-576.

Busch, N.E., 1977: Fluxes in the Surface Boundary Layer over the Sea. In *Modelling and Prediction of the Upper Layers of the Ocean*; E.B. Krauss, ed., Pergamon Press, Oxford, p. 72-91.

Busch, N.E. and H.A. Panofsky, 1968: Recent Spectra of Atmospheric Turbulence. Q.J.R. Meteorol. Soc. *94*: 132-48.

Denman, K.L. and M. Miyake, 1973: The behaviour of the mean wind, the drag coefficient, and the wave field in the open ocean. J. Geophys. Res. *78*: 1917-31.

Fissel, D.B., S. Pond and M. Miyake, 1977: Computation of Surface Fluxes from Climatological and Synoptic Data. Mon. Weather Rev. *105*: 26-36.

Friehe, C.A. and K.F. Schmitt, 1976: Parameterization of Air-Sea Interface Fluxes of Sensible Heat and Moisture by Bulk Aerodynamic Formulas. J. Phys. Oc. *6*: 801-09.

Garrett, J.R., 1977: Review of Drag Coefficients over Oceans and Continents. Mon. Weather Rev. *105*: 915-29.

Gill, G.C., 1975: Development and Use of the Gill UVW Anemometer. Boundary-Layer Meteorol. *8*: 475-95.

Hicks, B.B., 1972: Propeller Anemometers as Sensors of Atmospheric Turbulence. Boundary-Layer Meteorol. *3*: 214-28.

Hidey, G.M., 1972: A View of Recent Air-Sea Interaction Research. Bull. Am. Meteorol. Soc. *53*: 1083-1102.

Krauss, E.B., 1972: *Atmosphere-Ocean Interaction*. Oxford University Press, London, 275 pp.

Lumley, J.L. and H.A. Panofsky, 1964: *The Structure of Atmospheric Turbulence*. Interscience, New York, 239 pp.

Miyake, M., R.W. Stewart and R.W. Burling, 1970: Spectra and Cospectra of Turbulence over Water. Q.J.R. Meteorol. Soc. *96*: 138-43.

Miyake, M., M. Donelan and Y. Mitsuta, 1970: Airborne Measurements of Turbulent Fluxes. J. Geophys. Res. *75*: 4506-18.

Monin, A.S. and A.M. Yaglom, 1965; 1967: *Statistical Hydrodynamics, Vols. I and II.* Nauka, Moskow, 639 pp; 720 pp. (English translations updated and revised from MIT Press, J.L. Lumley, ed.)

Paquin, J.E. and S. Pond, 1971: The Determination of the Kolmogoroff Constants for Velocity, Temperature and Moisture from Second and Third Order Structure Functions. J. Fluid Mech. *50*: 257-69.

Phillips, O.M., 1972: Ocean Coupling and Response Times. In *Parameterizations of Sub-grid Scale Processes*. GARP publications series no. 8, p. 81-91.

Pond, S., 1975: The Exchanges of Momentum, Heat and Moisture at the Ocean-Atmosphere Interface. In *Numerical Models of Ocean Circulation*. Proceedings of U.S. National Academy of Sciences Symposium, pp. 26-38.

Pond, S., D.B. Fissel and C.A. Paulson, 1974: A Note on Bulk Aerodynamic Coefficients for Sensible Heat and Moisture Fluxes. Boundary-Layer Meteorol. *6*: 333-39.

Pond, S., G.T. Phelps, J.E. Paquin, G. McBean and R.W. Stewart, 1971: Measurements of the Turbulent Fluxes of Momentum, Moisture and Sensible Heat over the Ocean. J. Atmos. Sci. *28*: 901-17.

Roll, H.V., 1965: *Physics of the Marine Atmosphere*. Academic Press, New York, 426 pp.

Smith, S.D. and E.G. Banke, 1975: Variation of the Sea Surface Drag Coefficient with Wind Speed. Q.J.R. Meteorol. Soc. *101:* 665-73.

Smith, S.D., R.J. Anderson, E.G. Banke, E.P. Jones, S. Pond and W.G. Large, 1976: A Comparison of the Air-Sea Interaction Flux Measurement Systems of the Bedford Institute of Oceanography and the Institute of Oceanography, University of British Columbia. Bedford Institute of Oceanography Report Series BI-R-76-17. 41 pp.

Stewart, R.W., 1974: The Air-Sea Momentum Exchange. Boundary-Layer Meteorol. *6*: 151-67.

Appendix. Analysis of the Gill twin propeller vane anemometer.

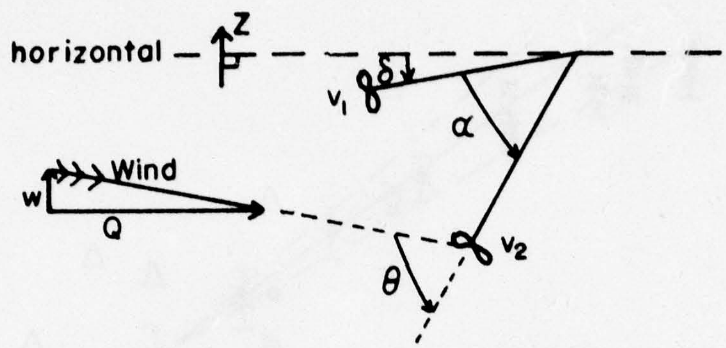

Fig. A.1. Sketch of propeller system to define angles; δ is tilt of v_1 propeller (tilt down taken to be positive), α is angle between propeller axes, nominally 60°, θ is angle of attack.

The propellers are vane-mounted which keeps their axes and the instantaneous wind vector in the same plane. If the propellers were cosine devices so that the axial velocity component v_i = total velocity times cosine of angle of attack, then

$$v_1 = Q\cos\delta + w\sin\delta$$

$$v_2' = Q\cos(\alpha+\delta) + w\sin(\alpha+\delta)$$

where $Q = \overline{Q} + q$, mean plus fluctuation of the horizontal velocity component and w is the vertical velocity component. Now $Q = [(\overline{U} + u)^2 + v^2]^{\frac{1}{2}}$ where $U = \overline{U} + u$ is the downstream component, v is the cross-stream component and $\overline{u} = \overline{v} = 0$. Thus expanding $Q = \overline{U} + u + \frac{v^2}{2\overline{U}}$ + higher order terms. $\sigma_v = (\overline{v^2})^{\frac{1}{2}} \simeq \overline{U}/10$ so the v^2 term is quite small and furthermore will be almost uncorrelated with u or w and may usually be neglected. In practice, we resolve Q into $\overline{U} + u$ and v using the wind direction indicated by the vane, but if the vane circuitry fails we can still obtain the Reynolds stress $\overline{qw}$ ($\overline{qw} = \overline{uw} + \frac{\overline{wv^2}}{2\overline{U}}$) but in near neutral conditions $\overline{w(w^2 + v^2 + u^2)} \sim u_*^3$ so $\overline{wv^2} < u_*^3$. The extra term $\lesssim 1/50\ u_*^3$ so $\overline{qw} = \overline{uw}$ within 1 or 2%). Note also that $\overline{Q} = \overline{U} + \frac{\overline{v^2}}{2\overline{U}} \simeq 1.005\ \overline{U}$ and for most purposes either may be used.

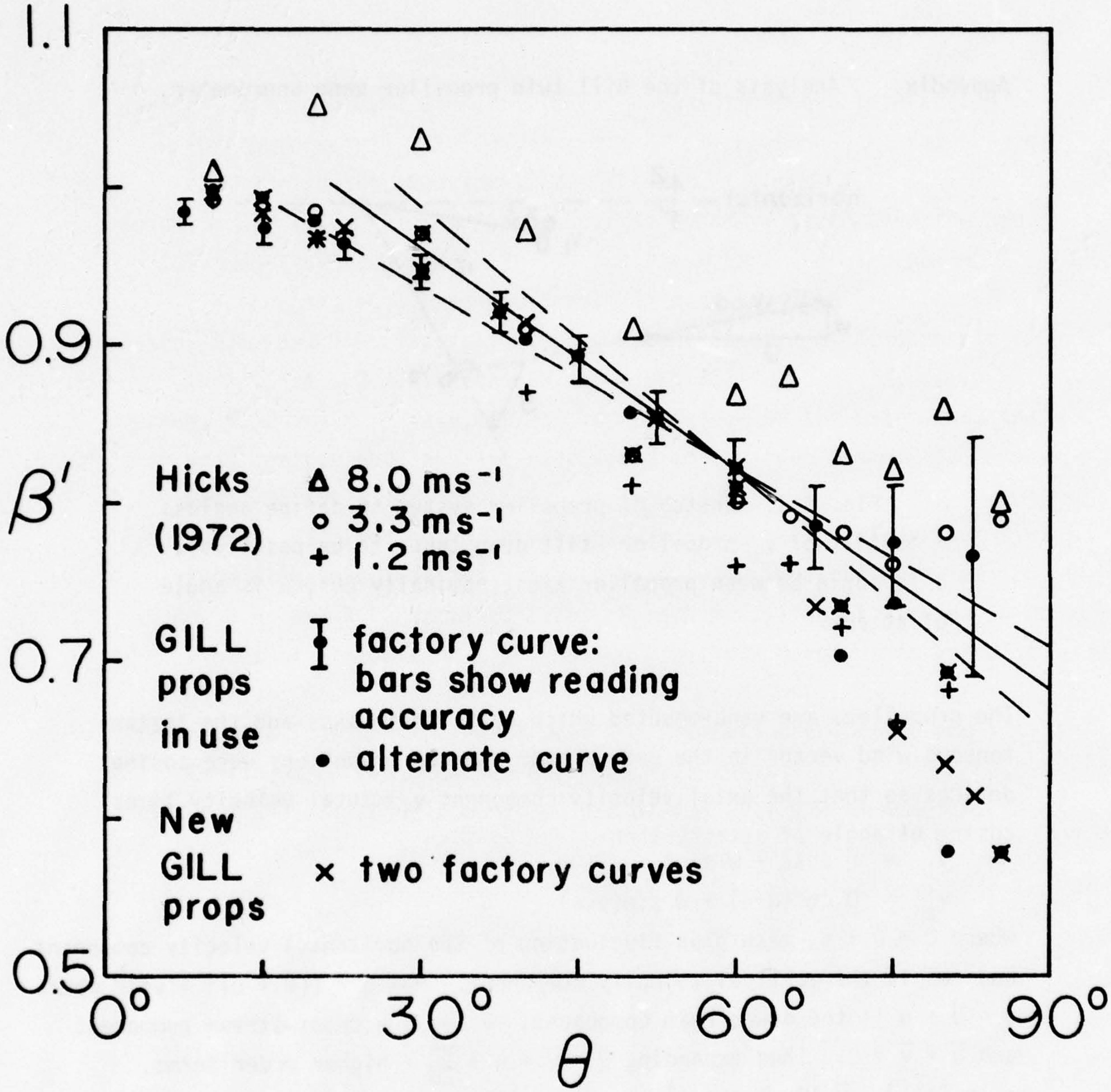

Fig. A.2. Deviation from cosine response; solid line $\beta' = 1.103 - 0.0047\,\theta$; dashed lines have slopes of -0.0038 and -0.0056.

For angles of attack greater than 10-20° the deviation from the cosine response must be taken into account. Since δ, the error angle if the axis of the v_1 propeller is not horizontal, will be small, the formula for v_1 should be sufficiently accurate. The observed value of v_2', v_2'', is found to be smaller than expected from cosine behaviour; $v_2'' = \beta' v_2'$. Figure A.2 shows values from four factory curves (R.M. Young Co.) as well as values from Hicks (1972). Hicks' values for 1.2 ms^{-1} are somewhat low as might be expected since below 1 ms^{-1} the output is lower than predicted from the linear relation between output voltage and wind speed for higher speed operation. His values for 8 ms^{-1} are somewhat high, exceeding 1.0 for θ = 10-30°, perhaps because of wake effects on the vertical shaft extension which was added to make the geometry more symmetric near 90°. In the range of 40-70° the slope is similar to the factory curves. We do not have such a shaft extension since we work near $\theta = 60°$. For any one set of points a linear relation in the range 35-70° or so fits reasonably well with some variation in the slope and intercept. Gill (1975) and the R.M. Young Co. (personal communication) do not find any variation of β' with flow speed up to 15 m/s provided it is sufficient to be in the linear operating range. From this figure we take $\beta' = 1.103 - 0.0047\,\theta$ where θ is the angle of attack in degrees and this formula is valid for θ from about 35-75°. For the v_2 propeller, $\theta = \alpha + \delta - \tan^{-1}(w/Q)$. Because w and Q are negatively correlated, θ is more likely to be $< \alpha + \delta$ than $> \alpha + \delta$. For example, if $w = -3\sigma_w \cong -0.18\,\overline{Q}$ (or $\overline{U}$ the mean of the downstream velocity component which differs from $\overline{Q}$ by about ½%) and taking q = 0 (although q is likely to be positive reducing the angle difference) $\theta \approx \alpha + \delta + 10°$. For $w = 3\sigma_w$ and $q = -3\sigma_q$ (where $\sigma_q \approx 1/10\,\overline{Q}$), $\theta \approx \alpha + \delta - 14°$. Now w and q (or u the downstream fluctuation) have nearly Gaussian probability distributions so the chance of $\tan^{-1} w/Q$ going outside the range +10° to -14° is very small (less than 1 in 500). The tilt angle, δ, which one of course tries to make as small as possible, should be a few degrees at worst. In practice we have found indicated δ's to be ±5 - 6° at most. Because of the uncertainty of the points in Figure A.2 the slope which is taken to be -0.0047 could range from -0.0038 to -0.0056 as shown by the dashed lines. The effect of these possible variations will be examined.

In order to do numerical calculations to show what results can be obtained we shall take $\alpha = 60°$. In practice, of course, we use the measured value for a particular instrument which we can obtain we believe to rather better than 1°.

Converting now to δ and $\tan^{-1}(w/Q)$ in radians and taking $\alpha = 60°$ for illustrative purposes

$$\beta' = 0.821\,[\,1 - 0.328\,(\delta - \tan^{-1}(w/Q))\,]\ .$$

It is convenient to multiply both sides of the equation for v_2'' by 1/0.821, that is, to include the deviation from the cosine response for the case $w = 0$ and $\delta = 0$ in the calibration, then

$$v_2 = v_2''/0.821 = \beta\,[\,Q\cos(\pi/3 + \delta) + w\sin(\pi/3 + \delta)\,]$$

where $\beta = 1 - 0.328\,(\delta - \tan^{-1}(w/Q))$. In the case $\alpha \neq 60°$ we use

$$\beta' = \beta'(\alpha)\,[\,1 - (0.269/\beta'(\alpha))(\delta - \tan^{-1}(w/Q))]$$

and take $v_2 = v_2''/\beta'(\alpha)$.

Now w/Q is fairly small so we can make the approximation $\tan^{-1}(w/Q) = w/Q$. This approximation neglects a term of order $(w/Q)^3$ but here we shall keep only terms to second order in small quantities (w/Q and δ) and show that they give sufficiently accurate results.

The tilt angle δ may vary slightly because of cross-stream fluctuations v (from existing data $\sigma_v \simeq \overline{U}/10$). For fluctuations in wind direction, ϕ, $\phi = \tan^{-1}(v/U) \simeq v/U$. δ will have its largest fluctuations when ϕ is such that δ is fluctuating about zero. Taking the maximum tilt to be 10° (although 5° is about as large as we have observed) $\delta = 10°\sin\phi \simeq 10° \times \phi \simeq 10°\ v/U$ and $(\overline{\delta^2})^{\frac{1}{2}} = \sigma_\delta \simeq 10°\ \sigma_v/\overline{U} \simeq 1°$. Thus in the worst case since v and hence δ will be approximately Gaussian we need to consider δ variations up to ±2° about the mean. We shall look at the effect of δ variations after considering the case when δ is constant.

Now we have

$$v_1 = Q\cos\delta + w\sin\delta$$

$$v_2 = [Q\cos(\pi/3 + \delta) + w\sin(\pi/3 + \delta)]\cdot[1 - 0.328\,\delta + 0.328\,w/Q]$$

Taking averages in time for a period of order ¼ hour or more, $\overline{w} << \overline{Q}$ so we assume $\overline{w} = 0$. Then

$$\overline{v}_1 = \overline{Q}\cos\delta$$

$$\overline{v}_2 = \overline{Q}[\cos(\pi/3+\delta)[1-0.328\,\delta] + 0.328\sin(\pi/3+\delta)\ \overline{w^2}/\overline{Q}^2]$$

correct to second order. The term in $\overline{w^2}/\overline{Q}^2$ is, taking $\sigma_w \simeq 0.06\ \overline{Q}$ and $\delta = 0$, 0.001 while the other term is 0.500. This term can probably be ignored compared to other errors (in calibration, D.C. drift, etc.). The procedure we use is to remove the Q part of v_2 by taking $v_2 - (\overline{v}_2/\overline{v}_1)v_1$ and then solve for w. When we ignore the $\overline{w^2}/\overline{Q}^2$ term we put about $-0.001\ Q$ and hence $-0.001\ u$ in $v_2 - (\overline{v}_2/\overline{v}_1)v_1$. If we correlate this with u then we add about $-0.001\ \overline{u^2}$ to $\overline{uw}$ or about 0.006 $\overline{uw}$ for an error of about ½%. For our four blocks of about 13 minutes each the ratio $\overline{v}_2/\overline{v}_1$ for an individual block varies from the mean for the four blocks by about $\pm$ 0.002 so the assumption $\overline{w} = 0$ should introduce a random error in $\overline{uw}$ of less than 1%. Note also that ignoring this term and higher order terms may give a w with a non-zero mean so it is important to remove the mean in w and/or in u or integrate the cospectrum leaving out the zero frequency value. If we calculate $\overline{uw}$ as $(\overline{U}+u) \times (w - .001(\overline{U}+u))$ we get $\overline{uw} - 0.001\ \overline{U}^2 - 0.001\ \overline{u^2}$ or about $\overline{uw}\ (1+0.6)$ which is a very serious error. Thus here, as in any Reynolds stress measurement, it is essential to remove the means. Actually the calculation is a little more complicated because with $\overline{v}_2/\overline{v}_1 = 0.501$ the calculated δ is not zero but -0.001 radians. Then u is calculated from $v_1 - \overline{Q} - w\tan\delta$ and is actually $u + .001\,w$ and $\overline{(w - .001\,u)\cdot(u + .001\,w)} = \overline{uw} - .001\ (\overline{u^2} - \overline{w^2}) \cong \overline{uw}\ (1 + .004)$ so the error is about ½ %.

Clearly for this procedure of removing the Q part of v_2 to work one must have good D.C. stability. We have been very careful about D.C. stability in designing our circuits using low temperature coefficient zener diodes as references for our power supplies and offset voltages. Before discussing the effects of offset errors further, because they produce apparent δ's which must be taken into account, let us first show examples when there are no errors.

Neglecting the $\overline{w^2}/\overline{Q}^2$ term for the moment we have

$$\overline{v}_2/\overline{v}_1 = \cos(\Pi/3+\delta)\,(1-0.328\,\delta)/\cos\delta$$
$$= (1-0.328\,\delta)\,(\cos\Pi/3\cos\delta - \sin\Pi/3\sin\delta)/\cos\delta$$
$$= \tfrac{1}{2}\,(1-0.328\,\delta)\,(1-\sqrt{3}\tan\delta)$$

Since δ is small, take $\tan\delta \simeq \delta$ which will give an expression correct to order δ^3. Then $2\overline{v}_2/\overline{v}_1 = [1-2.060\,\delta + 0.568\,\delta^2]$ which allows us to calculate δ from the observations of $\overline{v}_1$ and $\overline{v}_2$. The quadratic formula gives $\delta = 1.813 \pm \sqrt{1.528 + 3.521(\overline{v}_2/\overline{v}_1)}$. Since δ is clearly less than 1.813 radians we see that it is the root involving the $-\sqrt{\ }$ that is required.

$$\text{Now } v_2 = Q\cos(\Pi/3+\delta)\,(1-0.328\,\delta)$$
$$+\ w\,[\sin(\Pi/3+\delta)\,(1-0.328\,\delta) + 0.328\cos(\Pi/3+\delta)]$$
$$+\ 0.328\,w^2\sin(\Pi/3+\delta)/Q$$
$$v_1 = Q\cos\delta + w\sin\delta$$
$$\text{so } v_2 - (\overline{v}_2/\overline{v}_1)v_1 = w\,[[\sin(\Pi/3+\delta) - \cos(\Pi/3+\delta)\tan\delta][1-0.328\,\delta]$$
$$+\ 0.328\cos(\Pi/3+\delta)] + 0.328\,w^2\sin(\Pi/3+\delta)/Q$$
$$-\ 0.328\sin(\Pi/3+\delta)\,(\overline{w^2}/\overline{Q}^2)\,(Q\cos\delta + w\sin\delta)/\cos\delta\,.$$

Using $\sin(\Pi/3+\delta)\cos\delta - \cos(\Pi/3+\delta)\sin\delta = \sin\Pi/3$ we have

$$v_2 - (\overline{v}_2/\overline{v}_1)v_1 = w[(\sin(\Pi/3)/\cos\delta)(1-0.328\,\delta) + 0.328\cos(\Pi/3+\delta)]$$
$$+\ 0.328\,w^2\sin(\Pi/3+\delta)/Q$$
$$-\ 0.328\sin(\Pi/3+\delta)(\overline{w^2}/\overline{Q}^2)(Q\cos\delta + w\sin\delta)/\cos\delta\,.$$

Now the $\cos(\Pi/3+\delta)$ w term arises from the $\beta\ Q\cos(\Pi/3+\delta)$ term. Thus even to first order it is not sufficient to simply correct for the deviation from cosine response for the $w = 0$ angle of attack. Using the linear approximation and neglecting this term gives w's almost 20% too large. The uncertainty in the coefficient 0.328 will lead to some error but it is only about 3% as we shall show later. The final term can be neglected without serious error provided we remove the mean from u and/or w before calculating uw as noted before. The term in w^2 is kept because w^2 may be several times $\overline{w^2}$. However, with negligible error we can replace Q with $v_1/\cos\delta$ in this term. So the approximation we shall use is

$$v_2 - (\overline{v}_2/\overline{v}_1)v_1 = B\,w + A\,w^2/v_1$$

where $\overline{v}_2/\overline{v}_1$ observed is $\cos(\Pi/3+\delta)(1-0.328\,\delta)/\cos\delta + 0.328 \cdot \sin(\Pi/3+\delta)\,\overline{w^2}/\overline{Q}^2$

$$B = \sin(\Pi/3)(1-0.328\,\delta)/\cos\delta + 0.328\cos(\Pi/3+\delta)$$

$$A = 0.328\sin(\Pi/3+\delta)\cos\delta$$

and δ is calculated from $1.813 - \sqrt{1.528 + 3.521\,(\overline{v}_2/\overline{v}_1)}$

First, let us consider some examples where we calculate v_1 and v_2 without any approximations using assumed values of Q, w, and δ. Then we calculate w from the approximate formula. w_ℓ is the solution of $v_2 - (\overline{v}_2/\overline{v}_1)v_1 = B\,w_\ell$; w_q is the solution of the quadratic where with $B > 0$ the correct root involves $+\sqrt{b^2-4ac}$ in the equation $a\,w^2 + b\,w + c = 0$. We take $\overline{Q} = 10$ ms^{-1} $\sigma_q = 0.1\,\overline{Q} = 1$ ms^{-1} and $\sigma_w = 0.06\,\overline{Q} = 0.6$ ms^{-1}. Since u (and hence Q) are negatively correlated with w we take $\pm 2\sigma_w$ with $\mp 2\sigma_q$ and $\pm 3\sigma_w$ with $\mp 3\sigma_q$. These include about 96% and 99.7% of cases for Gaussian variables for C_D equal to 1.6×10^{-3}. When $C_D = 2.1\times10^{-3}$, then the $\pm 3\sigma$ case given includes 99% of cases provided σ_w/u_* and σ_q/u_* remain the same (as expected since observations over land give similar values).

Take $\delta = 10°$: $\overline{v}_2/\overline{v}_1$ observed = 0.3285; δ calculated is 10.02°. Calculated A and B are 0.3036 and 0.9411 (for $\delta = 10°$ A & B are 0.3035 and 0.9412).

w	Q	v_1	v_2	w_ℓ	w_q	$w_q + \frac{.0011v_1}{B}$
1.8	7	7.206	4.189	1.936	1.792	1.800
1.2	8	8.087	3.831	1.248	1.191	1.201
0	10	9.848	3.224	-0.012	-0.012	0.000
-1.2	12	11.609	2.709	-1.174	-1.215	-1.201
-1.8	13	12.490	2.473	-1.733	-1.818	-1.803

$w_\ell = w + (A/Bv_1)w^2$ and shows the expected distortion. Later we shall show that the effect of ignoring the quadratic term is reasonably small. w_q differs from w mainly by $-(0.0011/B)v_1$ which comes from neglecting the $\overline{w^2}/\overline{Q}^2$ term. q or u calculated from $v_1/\cos\delta - w \tan\delta$ will be in error by $10^{-4}\,u - 4 \times 10^{-4}\,w$ which is negligible. As noted before, the $10^{-3}\,u$ term in w calculated gives an error of about $+\frac{1}{2}\%$ in $|\overline{uw}|$.

Take $\delta = 0$: $\overline{v}_2/\overline{v}_1$ observed = 0.5010;

δ calculated is $-0.06°$	B = 1.031	A = 0.2839
for $\delta = 0°$	B = 1.030	A = 0.2841

w	Q	v_1	v_2	w_ℓ	w_q	$w_q + \frac{.0010\,v_1}{B}$
1.8	7	7.	5.476	1.911	1.785	1.792
1.2	8	8	5.285	1.239	1.191	1.199
0	10	10	5.000	-0.010	-0.010	0.000
-1.2	12	12.	4.799	-1.177	-1.211	-1.199
-1.8	13	13	4.718	-1.741	-1.811	-1.798

W_q error is $-0.001\,v_1$. The q error is $10^{-6}\,u + 10^{-3}\,w$ and $\overline{uw}$ error is $-10^{-3}(\overline{u^2} - \overline{w^2}) < \frac{1}{2}\ \%$.

Take $\delta = -10°$: $\overline{v}_1/\overline{v}_2$ observed = 0.6910;

δ calculated is $-10.13°$	B = 1.142	A = 0.2469
for $\delta = -10°$	B = 1.141	A = 0.2474

w	Q	v_1	v_2	w_ℓ	w_q	$w_q + \frac{.0009\,v_1}{B}$
1.8	7	6.581	6.700	1.885	1.781	1.786
1.2	8	7.670	6.705	1.230	1.190	1.196
0	10	9.848	6.796	-0.008	-0.008	0.000
-1.2	12	12.026	6.961	-1.181	-1.207	-1.198
-1.8	13	13.115	7.062	-1.752	-1.805	-1.795

The q error is $-5 \times 10^{-4}\,u + 2 \times 10^{-3}\,w$. Error in $\overline{uw}$ calculated $< \frac{1}{2}\ \%$.

Clearly given a steady value of δ, an accurate α, good D.C. stability, accurate calibrations and an accurate formula for β', we can calculate w with good accuracy and with negligible contamination with u, the downstream velocity component. Removal of u in the calculated w is essential to avoid large errors in uw in any method of obtaining uw and the procedure is designed specifically to do this removal as well as possible. Note that even at 5 ms^{-1} and $\delta = 10°$, $v_2 > 1$ ms^{-1} so that we stay in the linear range of the propeller's output, the original intent of using $\alpha \simeq 60°$ rather than 90°. At higher turbulence levels (e.g. over fairly rough land) where δ might become as large as 10°, it would probably be best to use $\alpha \simeq 50°$. A smaller α would decrease the relative importance of the quadratic term somewhat but increase the uncertainty in B and δ because of the uncertainty of the slope in β'.

Let us now look at how various errors affect the calculated w. Since w is also used in calculating u (or q) from v_1 these errors may propagate into u and the calculated uw so the effect on uw must be examined as well. w is obtained from $a w^2 + b w + c = 0$ where $c = -(v_2 - (\overline{v}_2/\overline{v}_1)v_1)$, $b = B$ and $a = A/v_1$. Now $|4ac| \ll b$ so we can expand $w = (-b + \sqrt{b^2 - 4ac})/2a$. to give $w \cong -c/b - (a/b)(c/b)^2$ in order to do our error analysis. Note that this expansion is equivalent to using w_ℓ in the quadratic term to get an approximate solution for w

$$w_\ell = -c/b \quad \text{and} \quad w = w_\ell - (a/b)w^2 .$$

Calculate $w' = w_\ell - (a/b)w_\ell^{\,2} = w + (a/b)w^2 - (a/b)(w^2 + (2a/b)w^3 + (a^2/b^2)w^4)$. $w' = w + O(w^3)$ so w' is also a second order accurate solution and could be used. In practice w_q the solution to the quadratic is better containing smaller w^3 terms than w'. However, in analyzing for the error, δw, due to variations in a, b, c the second order accurate w' solution is easier to use and should be of sufficient accuracy.

$$\delta w = -\frac{c}{b}\cdot\frac{\delta c}{c} + \frac{c}{b}\cdot\frac{\delta b}{b} - \frac{a}{b}(c/b)^2\frac{\delta a}{a} - \frac{2a}{b}(c/b)^2\frac{\delta c}{c} + \frac{3a}{b}(c/b)^2\frac{\delta b}{b}$$

The first two terms came from shifts in w_ℓ due to c and b changes while the final three are associated with changes to the 'correction' term $-(a/b)w_\ell^{\,2}$. As this term is quite small (< 10% of w_ℓ) the three final terms will generally be of secondary importance. If we calculate δw from $(\partial w/\partial a)\delta a + (\partial w/\partial b)\delta b + (\partial w/\partial c)\delta c$ then the terms above are the largest terms in an expansion of this more exact expression.

Errors in α

Suppose α is actually 62° instead of 60°. v_2 will then be smaller than expected because we have included $\beta'(60)$ in the calibration, not $\beta'(62)$; the factor is 0.9886. With $\delta = 0$, $\overline{v}_2/\overline{v}_1$ observed is 0.9886 cos(62) + 0.328 sin(62) $\overline{w^2}/\overline{Q}^2$ = 0.4651. δ calculated is 1.96° because in the formula used to calculate δ the $1 - 0.328\,\delta$ factor accounts almost exactly for the $\beta'(62)/\beta'(60)$ factor (if the $\overline{w^2}/\overline{Q}^2$ term is subtracted from $\overline{v}_2/\overline{v}_1$ then δ calculated is 2.02°). Thus any error in α appears as an apparent tilt angle δ.

A should be 0.9886 · (.328/0.9886) sin62° = 0.2896,
calculated to be 0.328 sin(61.96°) cos(1.96°) = 0.2893;

B should be 0.9886 sin62° + 0.328 cos62° = 1.027,
calculated to be 1.011.

There is no error in c as it is taken as given; there is a small error in a ($\delta a/a \simeq 0.015$) but as it is in a second order correction the error in w is 2×10^{-3} at most and can be ignored. The main error is in b (= B). Since B used is too small, w will be too large by about 1½%.

w	Q	v_1	v_2	w_ℓ	w_q	$w_q + \frac{.001\, v_1}{B}$
1.8	7	7	5.222	1.945	1.811	1.818
1.2	8	8	4.995	1.261	1.208	1.216
0	10	10	4.641	-0.010	-0.010	0.000
-1.2	12	12	4.372	-1.196	-1.232	-1.220
-1.8	13	13	4.258	-1.768	-1.843	-1.830

w is a little large as predicted and contains -0.001 u. However, because we take u to be the fluctuating part of $v_1/\cos\delta - w\tan\delta$ and v_1 actually has no w in it (the true $\delta = 0$) we get 1.0006 u - 0.034 w. $\overline{uw}$ calculated $(1.015\,w - 0.001\,u)(1.0006\,u - 0.034\,w) = 1.016\,\overline{uw} - .001\,\overline{u^2} - 0.035\,\overline{w^2}$. With $\sigma_w = 1.5\,u_*$, $\sigma_u = 2.5\,u_*$, $|\overline{uw}|$ calculated is 10% too large. Thus while we have gotten the u out of w pretty well we have left some w in the calculated u. This problem is not peculiar to this system. An error in the angle between the axes along which components are resolved will lead to the same problem in any system and the error will be similar assuming one is careful to use $\bar{w} = 0$ to remove any u signal from the calculated w. The error is a little worse here because the w calibration is also affected a little ($\sim 1.5\%$). For a one degree error in α the $\overline{uw}$ error is about 5%; for a system for which only the w in u causes an error (e.g. a sonic anemometer) the error would be 4%. We believe we can measure α to rather better than 1° but to be on the safe side we must consider there to be a possible error of up to ± 5% from α errors. Since $\bar{U}$ is not appreciably affected the error in C_D is also similar.

Offset errors

We have been careful to make these very small as noted earlier, and we expect them to be similar in both v_1 and v_2 in % terms so that they cancel. At 5 m/s an offset error corresponding to ± 2 bits (i.e. ± 5 mv) is about 1/200 in v_1 and 1/150 in v_2. Suppose the worst, that these offsets occur with opposite signs. With $\bar{Q} = 5\ ms^{-1}$ and $\delta = 0$ for v_1 we add $0.025\ ms^{-1}$ to the values, and for v_2 we add $-0.015\ ms^{-1}$. $\bar{v}_2/\bar{v}_1 = 2.485/5.025 + .001 = .4955$ instead of 0.5010, δ calculated = 0.25°. As well as a small offset error in w_q, which we ignore since means are removed, we get $w + 0.0045\,u$. A calculated is 0.2848, correct A is 0.2841. B calculated is 1.028; B correct is 1.030. The main error is due to adding some u to w. uw calculated is $(w + 0.0045\,u)\ (u - .0044\,w) = uw + .0045\,(u^2 - w^2)$, so $|\overline{uw}|$ is about 2% too small. $\bar{U}^2$ is about 1% high and C_D about 3% too small. If the errors are opposite $\bar{v}_2/\bar{v}_1 = 0.5065$, w calculated $= w - .065\,u$, $\delta = -0.36°$, u calculated $= u + .0063\,w$. Error is $-0.0065(u^2 - w^2)$; $|\overline{uw}|$ is about 2.5% too large and C_D about 3.5% too large. Thus at 5 ms^{-1} the error is about 2.5%, at 10 ms^{-1} about 1% in $\overline{uw}$ and perhaps 2% in C_D, and lower at higher speeds. Note that the apparent δ is such as to add a little w to the calculated u which helps to reduce the error. In fact the offset errors due to thermal drift are in the same direction so the actual errors are ½ or less than these worst case values.

Calibration errors

For one propeller relative to the other, the calibrations are probably accurate to about ± 1%. Overall, based on our own checks amongst others, they should certainly be better than ± 2%. If both propellers are 2% high or low then the effect cancels in calculating δ, A, B; w and u will both be 2% high or low together; $\overline{uw}$ will be ± 4% but in calculating C_D the error cancels out and C_D is unaffected. If v_1 is 2% high while v_2 is 2% low and δ true = 0, then $\overline{v}_2/\overline{v}_1$ = 0.4814. In taking $v_2 - (\overline{v}_2/\overline{v}_1)v_1$ we are still left with - 0.001 u; using the observed ratio still gets the u out of w in the same way as before. w is of course 2% too small due to the calibration error, but B calculated is 1% low so w is only 1% low, u is 2% too big, δ apparent is 1.04°, so u apparent is 1.02 u - .018 w and uw as calculated is $1.01\,uw - .001\,u^2 - .018\,w^2$ and is about 5% too large in size; again the effects on C_D tend to cancel and it is only 1% too large.

If v_1 is 2% low while v_2 is 2% high and δ true = 0, then $\overline{v}_2/\overline{v}_1$ = 0.5214, δ calculated is - 1.18°; B is 1% high and w is 1% high; u is 2% low, but has 0.021 w in it so uw calculated is (.98 u + .021 w)(1.01 w - .001 u) $= 0.99\,uw + 0.021\,w^2 - .001\,u^2$. $\overline{uw}$ is about 5% too small in size but since $\overline{U}$ is 2% low, C_D is only about 1% low.

Errors in the $\beta'(\theta)$ relation

From Fig. A.2 it is clear that some variation in this function is possible. To examine the effects let us assume that the relation used so far is correct and see what happens when we use some other $\beta'(\theta)$ in calculating w, uw and C_D. Suppose we think that $\beta'(60)$ the intercept is 0.84 instead of 0.821, then the calculated v_2's will be too small by 0.821/0.84 = 0.977 and so will $\overline{v}_2/\overline{v}_1$ by the same amount. For true δ's of 10, 0, -10 the calculated δ's are: 10.49, 0.59, -9.32. $v_2 - (\overline{v}_2/\overline{v}_1)v_1$ will be 2.3% low and will contain - 0.001 u as before. Because of the apparent δ, B will also be too low by about 0.6% and A will be about 0.6% high. The change in A can be ignored since it occurs in a small correction term. Thus |w| calculated will be about 1.7% too small. At the same time, we introduce some w into the calculated u (-.9, -1.0 and -1.2% for δ = 10, 0, -10°). So $|\overline{uw}|$ calculated has an error of -1.7% from small w, + 0.6 % from u in w and + 1.9 to 2.5% from w in u due to the apparent δ. Thus $|\overline{uw}|$ is 0.8 to 1.5% too large and so is C_D. If the assumed intercept is 0.80 then $|\overline{uw}|$ and C_D are almost unchanged because the effect of the $-0.001\,u$ in w cancels the intercept change. Our original calculations were based on the curve with the 0.82 intercept. When the other data are plotted it appears that 0.81 might be better in which case our $|\overline{uw}|$'s are about ½% too small, neglecting the $-0.001\,u$ in the calculated w. However, neglecting the $\overline{w^2}/\overline{Q^2}$ term in $\bar{v}_2/\bar{v}_1$ tends to make $|\overline{uw}|$ about ½% too large and compensates. The effect of this possible error in the intercept is about ± 1% for intercept variations of ± 0.04 and $|\delta| < 5°$.

With the intercept unchanged, variations in the slope used in the calculations do not change $\bar{v}_2/\bar{v}_1$ but do change A, B and the apparent δ. With the slope variations shown in Figure A.2 the 0.328 coefficient in the equations may vary from 0.265 to 0.391. A then also varies by ± 20%. The effect of using the wrong A is then to leave about 20% of $(A/Bv_1)w^2$ or second harmonic distortion in the calculated w. As we shall show later, the effect of ignoring the whole second harmonic (w^2) term is small so if 20% of it is left in it should not matter. Suppose the correct coefficient is 0.328 but we assume it to be 0.265, then the δ equation becomes $1-(\sqrt{3}+0.265)\delta+0.265\sqrt{3}\,\delta^2 = 1-1.997\,\delta + 0.459\,\delta^2$. For an actual $\delta = 10°$, δ calculated is 10.38°, B calculated is 1.5% low, making $|w|$ calculated 1.5% too large. u calculated is actually $u-.007\,w$ so $|\overline{uw}|$ calculated is 3% too large and so is C_D (actually 3.5% considering the u in w effect). At $\delta = 0$ only the effect on B needs to be considered; it is 3% low and $|w|$ and $|\overline{uw}|$ are 3% high. For $\delta = -10°$, δ calculated is -10.63°, B is 4% low and $|w|$ 4% high, but u calculated is $u + 0.011\,w$ so $|\overline{uw}|$ is in error by + 2%.

If we assume the slope coefficient is 0.391 instead of 0.328, the δ equation is $1-2.123\,\delta + 0.677\,\delta^2$. For $\delta = 10°$, δ calculated is 9.79°, B is 1.5% high and $|w|$ 1.5% low; u calculated is $u+0.004\,w$, so $|\overline{uw}|$ is 2.5% too small from the slope effect and the $-.001\ u$ in w reduces this to < 2%. At $\delta = 0$, B is 3% high and $|w|$ 3% low; $|\overline{uw}|$ is 2.5% low including the effect of the $-0.001\,u$ in w. For $\delta = -10°$ δ calculated is -9.78, B is 4% high and $|w|$ 4% low; u calculated is $u-0.004\,w$ so $|\overline{uw}|$ is 2.5% low including the u in w effect.

If the slope and intercept both change the effects should be additive. From Fig. A.2 a low slope would tend to go with a high intercept and vice versa. At $\delta = 0$, we get a total error of $+\frac{1}{2}\%$ from the intercept, +3% from slope, $+\frac{1}{2}\%$ from the u in w for a total of 4%. By calculation, $|w|$ is too small by 2.3% from the change in $v_2 - (\overline{v}_2/\overline{v}_1)v_1$, δ calculated is 0.61°, B is 3.5% too small, so w is 1.2% too large and contains $-.001u$. u calculated is $u - .011w$ so $|\overline{uw}|$ is +1.2% + 0.6% + 2.2 = 4% too large, which agrees. For a high slope and low intercept at $\delta = 0$, $|\overline{uw}|$ is $-\frac{1}{2}\%$ from the intercept, $+\frac{1}{2}\%$ from the u in w and -3% from the slope, for a total of -3%.

Thus, overall the error in $\beta'(\theta)$ should lead to an error of about ± 3%. As the slope for any given data set (where the experimental error does not cause a lot of scatter, i.e. beyond about 70°) seems to be well within the limits which we have used to calculate errors, the error is probably less than ± 3%.

Errors due to fluctuations in δ

$\delta = \delta_o \cos(\phi - \phi_o)$ where ϕ is the wind direction and δ has its maximum δ_o when $\phi = \phi_o$. Taking $\overline{\phi}$ to be in the direction of $\overline{U}$ the mean downstream component

$$\phi - \overline{\phi} = \sin^{-1} v/Q; \quad \sin(\phi - \overline{\phi}) = v/Q$$

$$\cos(\phi - \overline{\phi}) = 1 - v^2/2Q^2 + O(v^4/Q^4)$$ and the term $O(v^4/Q^4) \le 0.001$

99.7% of the time if v is Gaussian, so we neglect it.

$$\delta = \delta_o\{\cos(\phi - \overline{\phi})\cos(\phi_o - \overline{\phi}) + \sin(\phi - \overline{\phi})\sin(\phi_o - \overline{\phi})\}$$

$$= \delta_o\{\cos(\phi_o - \overline{\phi})(1 - v^2/2Q^2) + \sin(\phi_o - \overline{\phi})(v/Q)\}$$

$$\overline{\delta} = \delta_o\{\cos(\phi_o - \overline{\phi})(1 - \overline{v^2}/2\overline{Q}^2 + \text{higher order terms})$$

Fluctuations in $\delta = \delta - \overline{\delta} = \delta_o\{\cos(\phi_o - \overline{\phi})(\overline{v^2}/2\overline{Q}^2 - v^2/2Q^2) + \sin(\phi_o - \overline{\phi})(v/Q)\}$.
When $\phi_o - \overline{\phi} = 0$, $\overline{\delta} = \delta_o(1 - .005)$ so the difference between $\overline{\delta}$ and $\delta_o\cos(\phi_o - \overline{\phi})$ is about 0.05° at worst.

Note that the δ fluctuations have both a linear and a quadratic term in v/Q.

Consider the Q part of v_1 with $\delta = \overline{\delta} + \delta'$

$$Q(\cos\overline{\delta}\cos\delta' - \sin\overline{\delta}\sin\delta')$$

$$\overline{Q\cos\delta'} = \overline{Q}\,[1 - \delta_o^2\sin^2(\phi_o - \overline{\phi})\,\overline{v^2}/2\overline{Q}^2] \text{ to second order}$$

$$= \overline{Q}\cos\sigma_\delta$$

$$\overline{Q\sin\delta'} = 0 \text{ to second order}$$

We see that although Q and δ' are correlated it is at such high order that we may ignore it.

$$v_2 = Q\,[\cos(\pi/3 + \overline{\delta})\cos\delta' - \sin(\pi/3 + \overline{\delta})\sin\delta'\,][1 - 0.328(\overline{\delta} + \delta')]$$
$$+ f(w)$$

$$\overline{v_2} = \overline{Q}\cos(\pi/3 + \overline{\delta})\cos\sigma_\delta\;(1 - 0.328\,\overline{\delta})$$
$$- \overline{Q}\sin(\pi/3 + \overline{\delta})\cdot 0.328\,\sigma_\delta^{\,2} + O(\overline{w^2}/\overline{Q})$$

but the second term is 0.0001 $\overline{Q}$ which is negligible so we get the correct $\overline{v}_2/\overline{v}_1$ and $\overline{\delta}$ even if δ is fluctuating. In solving for w, $\overline{v}_2/\overline{v}_1$, $\overline{\delta}$, A and B are the same as if δ were fixed but as δ changes, $v_2 - (\overline{v}_2/\overline{v}_1)v_1$ will contain extra fluctuations. Consider first the part involving Q

$$v_1 = Q(\cos\overline{\delta}\cos\delta' - \sin\overline{\delta}\sin\delta')$$

$$v_2 = Q\{\cos(\pi/3 + \overline{\delta})\cos\delta' - \sin(\pi/3 + \overline{\delta})\sin\delta'\}\{1 - 0.328(\overline{\delta} + \delta')\}$$

$$v_2 - (\overline{v}_2/\overline{v}_1)v_1 = Q\{\cos(\pi/3 + \overline{\delta})\cos\delta' \cdot (-0.328\,\delta')$$
$$- \sin(\pi/3 + \overline{\delta})\sin\delta'\;(1 - 0.328(\overline{\delta} + \delta'))$$
$$+ \overline{v}_2/\overline{v}_1\sin\overline{\delta}\;\sin\delta' - 0.001\}$$

Now this is to be correlated with u or q but they are unrelated to δ' to second order. The largest term (other than the $-0.001\,u^2$ associated with neglecting the $\overline{w^2}/\overline{Q}$ in $\overline{v}_2$) which will be added to uw is $0.328\sin(\pi/3 + \overline{\delta})\;\overline{\delta'^2}.\;\overline{u^2} \leq 10^{-4}\overline{u^2}$ which is completely negligible. The fluctuations in w are of order ± 0.04 Q for $\delta_o = 10°$ and $\sigma_\delta = 1°$ which are not so small but the average effect is very small. Likewise, there will be a variation in the calculated w involving $w\delta'$ and $w\delta'^2$ terms but these will also have a completely negligible effect on the calculated $\overline{uw}$.

Non-cosine response of the v_1 propeller

Up to about 10° the deviation from cosine response is undetectable within experimental error. With $|\delta| < 5°$ the angle of attack stays within 10° almost all the time. However, with larger tilt errors of 10 - 15° the effect may be of importance. From Fig. A.2 near $\theta = 15°$, $\beta' = 1 - 0.038\,\theta$ with θ in radians, is a possible fit and v_1 will be

$$v_1 = (Q\cos\delta + w\sin\delta)(1 - 0.038\,|\delta - w/Q|)$$

Suppose this relation holds even when $\delta = 0$ and consider the situation when $\delta = 0$

$$v_1 = Q - 0.038\,|w|$$
$$\overline{v}_1 = \overline{Q} - 0.038\,\overline{|w|}$$

Now w is approximately Gaussian, so $\overline{|w|} \simeq \sigma_w/\sqrt{\Pi} \simeq 0.06\,\overline{Q}/\sqrt{\Pi}$ and $v_1 = 0.999\,\overline{Q}$. $\overline{v}_2/\overline{v}_1$ is now 0.5015 and δ calculated is $-0.08°$. The effect on A and B is about 0.1% which can be ignored. w calculated is $w - 0.0015\,u + 0.019\,|w|$ while u calculated is $u + 0.0015\,w - 0.038\,|w|$ and $\overline{uw}$ calculated is $\overline{uw} - .0015(\overline{u^2} - \overline{w^2}) - .0007\,\overline{w}^{\,2}$, since $|w|^2 = w^2$, $\overline{w|w|} = 0$ and $\overline{u|w|}$ is small and assumed zero. The error in $|\overline{uw}|$ is about 0.8% and the error in $C_D \simeq +1\%$. If $|\delta|$ is larger than 10° or so then $|\delta - w/Q|$ is $\delta - w/Q$ for $\delta > 0$ and $-\delta + w/Q$ for $\delta < 0$. There is rather more w in v_1 than included in the formulae given earlier and it may cause fairly large errors.

Consider $\delta = 10°$, then taking

$$v_1 \simeq (Q\cos\delta + w\sin\delta)\,(1 - 0.038(\delta - w/Q))$$
$$\overline{v}_1 = \overline{Q}\cos\delta\,(1 - 0.038\,\delta) + 0.038\sin\delta\,\overline{w^2}/\overline{Q}$$

The second term is $\simeq 2 \times 10^{-5}\,\overline{Q}$ and may be ignored. $\overline{v}_1 = \overline{Q}\cos\delta \times 0.0.993$ and is 0.7% smaller than if the possible non-cosine effect is ignored. $\overline{v}_2/\overline{v}_1$ is larger and δ calculated is 9.89°. The error in B is about 0.1% and in A even less. $v_2 - (\overline{v}_2/\overline{v}_1)v_1$ is as calculated in the simpler formula except for the extra w term which is $-0.012\,w$ and the calculated w is 1.2% too small. u as calculated is $0.993\,u + 0.04\,w$ and $\overline{uw}$ calculated is $(0.988\,w - 0.001\,u)(0.993\,u + 0.04\,w) = 0.981\,\overline{uw} - .001\,\overline{u^2} + 0.04\,\overline{w^2}$, or about

10% too small in size; C_D is 9% too small.

When $\delta = -10°$, $|\delta - w/Q| = 10° + w/Q$ $\overline{v}_1$ is $0.993\,\overline{Q}\cos\delta$ as for $\delta = +10°$. In $v_2 - (\overline{v}_2 - \overline{v}_1)v_1$ the extra term is $+0.026\,w$. δ calculated is -10.38° making B 0.4% too large, so the net effect is that w is 2.2% too large. u as calculated is 0.993 u - .030 w. $\overline{uw}$ as calculated is (1.022w - .001u) (0.993 u - .030 w) which is about 9% too large; C_D is about 10% too large.

From the experimental data it is difficult to determine how important this possible error may be. For small $|\delta|$, say less than 2°, not only is the deviation from cosine response likely to be smaller, but also the contribution from the extra w term in v_1 tends to cancel as it does when $\delta = 0$ where it is a $|w|$ term. If one has a large body of data then one can look for systematic differences between $\delta = 0$, $\delta \simeq 4-5°$ and $-\delta \simeq 4-5°$ in the data set and we shall attempt to do so in the analysis of the data we have obtained. Some further wind tunnel work would probably be helpful too in the range $\theta = 0$ to $\pm 20°$.

<u>The importance of the quadratic term</u>

It is a fairly simple matter to solve for w_q. However, if the linear approximation is adequate, operations could be done on the Fourier coefficients of v_1 and v_2 which have to be found to correct for instrument response and then inverse transformed to calculate w_q.

$$w_\ell = w + aw^2, \text{ where } a = A/(BQ\cos\delta)$$

$$\overline{w_\ell^{\,2}} = \overline{w^2} + 2\overline{aw^3} + \overline{a^2w^4}$$

Put $Q \simeq \overline{U} + u$

$$\overline{w_\ell^{\,2}} = \overline{w^2} + [2A/(B\cos\delta\,\overline{U})][\overline{w^3} - \overline{uw^3}/\overline{U}] + (A/(B\cos\delta))^2\,\overline{w^4}/\overline{U}^2$$

$\overline{w^3}$ will be small compared to $\sigma_w^{\,3}$ and $\overline{w^4} \sim 3\,\sigma_w^{\,4}$. $A/B\cos\delta$ is 0.33 to 0.22 for $\delta = +10$ to $-10°$. The w^3 term $\sim 2/3\,(\sigma_w/\overline{U})\cdot(\sigma_w^{\,2})\cdot(\overline{w^3}/\sigma_w^{\,3})$. $\sigma_w/\overline{U} \sim 0.06$ and $\overline{w^3}/\sigma_w^{\,3}$ will certainly be less than 1/10 $\therefore$ the w^3 term $< 0.004\,\overline{w^2}$ and can be neglected. Even if u and w^3 are perfectly correlated the $\overline{uw^3}$ term < 0.004 $\overline{w^2}$. The $\overline{w^4}$ term < 0.0004 $\overline{w^2}$. Thus, $\overline{w_\ell{}^2} = \overline{w^2}$ with less than 1% error. The spectra of the two should also be similar except perhaps where the w spectrum is very small.

Consider $u_\ell = v_1/\cos\delta - w_\ell \tan\delta - (\overline{U} + (v^2/2\overline{U}))$

$$= u - A/(B\cos\delta)\cdot\tan\delta\cdot(w^2/\overline{U})\ [1 - u/\overline{U}] + \text{higher order terms}$$

$$\overline{u_\ell{}^2} = \overline{u^2} - (2A\tan\delta)/(B\cos\delta)\ (\overline{uw^2}/\overline{U}) + \text{higher order terms}$$

For $|\delta| < 10°$ the second term is $\leq 0.005\ \overline{u^2}$ even if u and w^2 are perfectly correlated. Thus u_ℓ is a good approximation for u.

Finally, consider $\overline{u_\ell w_\ell}$

$$= \overline{(w + (A/(B\cos\delta))\ (w^2/Q))\ (u - ((A\tan\delta)/(B\cos\delta\ Q))w^2)}$$

$$= \overline{uw} + [A/(B\cos\delta)]\ \overline{[uw^2/Q - (w^3\tan\delta)/Q]}$$

The largest error term is $A/(B\cos\delta\cdot\overline{Q})\ \overline{uw^2}$. For perfect correlation this term would be about 7% of $|\overline{uw}|$ but the correlation will be much less than 1 so the error is probably negligible.

At present we are calculating w_q not w_ℓ but we plan to compare results from calculations using both with real data to check that the use of w_ℓ is adequate as it appears to be.

Because of slope errors about 20% of the $(A/B\cos\delta)(w^2/Q)$ term may be left in even when we calculate w_q but as the effect of the whole term is small leaving in 20% of it can be ignored.

UNCLASSIFIED

SECURITY CLASSIFICATION OF THIS PAGE (When Data Entered)

REPORT DOCUMENTATION PAGE		READ INSTRUCTIONS BEFORE COMPLETING FORM
1. REPORT NUMBER 32	2. GOVT ACCESSION NO.	3. RECIPIENT'S CATALOG NUMBER
4. TITLE (and Subtitle) A system for remote measurements of air-sea fluxes of momentum, heat and moisture during moderate to strong winds.		5. TYPE OF REPORT & PERIOD COVERED Manuscript Report
		6. PERFORMING ORG. REPORT NUMBER 32
7. AUTHOR(s) S.Pond and W.G. Large		8. CONTRACT OR GRANT NUMBER(s) N00014-76-C-0446 NR 083-207
9. PERFORMING ORGANIZATION NAME AND ADDRESS Institute of Oceanography University of British Columbia Vancouver, B.C., Canada V6T 1W5		10. PROGRAM ELEMENT, PROJECT, TASK AREA & WORK UNIT NUMBERS
11. CONTROLLING OFFICE NAME AND ADDRESS Office of Naval Research ONR Code 481 NSTL Station, Mississippi 39529		12. REPORT DATE March 1978
		13. NUMBER OF PAGES
14. MONITORING AGENCY NAME & ADDRESS(if different from Controlling Office)		15. SECURITY CLASS. (of this report)
		15a. DECLASSIFICATION/DOWNGRADING SCHEDULE

16. DISTRIBUTION STATEMENT (of this Report)

Unlimited

DISTRIBUTION STATEMENT A
Approved for public release;
Distribution Unlimited

17. DISTRIBUTION STATEMENT (of the abstract entered in Block 20, if different from Report)

18. SUPPLEMENTARY NOTES

19. KEY WORDS (Continue on reverse side if necessary and identify by block number)

air-sea interaction measuring system; anemometers; low power digital recording systems.

20. ABSTRACT (Continue on reverse side if necessary and identify by block number)

The report describes the methods employed, the sensors used for temperature, humidity and velocity and the digital recording systems. A summary of the field measurements made and some preliminary results are given. A detailed analysis of the GILL twin propeller-vane anemometer is presented in the appendix.